POLITECNICO
MILANO 1863

SCUOLA DI INGEGNERIA INDUSTRIALE
E DELL'INFORMAZIONE

Projection Continuation for Singularity Detection of Redundantly Constrained Multibody System Dynamics

Tesi di Laurea Magistrale in
Aeronautical Engineering - Ingegneria Aeronautica

Author: **M Jihad Ummul Quro**

Student ID: 974843
Advisor: Prof. Pierangelo Masarati
Academic Year: 2022-23

Abstract

One approach to solving multibody system dynamics cases is to use a minimal coordinate set via QR factorization. This method provides the trajectory of the physical coordinates. However, the generalized coordinates corresponding to the motion of the system are discontinuous. A continuation algorithm is thus proposed to maintain the evolution of generalized coordinates by preserving the spatial continuity of the system coordinates.

In this thesis, the method will be used to evaluate the singularity conditions that may occur in the system during its motion. A mechanical singularity is a critical condition where the system can begin to perform a different behavior from the original motion. In addition, this approach is also used to solve cases where there are redundant constraints on the system mechanism, meaning some constraints are not independent. Several examples of 4-bar mechanisms and their modifications are presented in this thesis to see the implementation of the minimal coordinate set approach with and without continuation to detect when singularity configuration occurs and when the system has redundant constraints.

Keywords: Minimal Coordinate Set, QR Factorization, Continuation Algorithm, Singularity Configuration, Redundant Constraint

Abstract in lingua italiana

Un approccio alla risoluzione dei casi di dinamica dei sistemi multicorpo consiste nell'utilizzare un set minimo di coordinate tramite la fattorizzazione QR. Questo metodo fornisce la traiettoria delle coordinate fisiche. Tuttavia, le coordinate generalizzate corrispondenti al moto del sistema sono discontinue. Viene quindi proposto un algoritmo di continuazione per mantenere l'evoluzione delle coordinate generalizzate preservando la continuità spaziale delle coordinate del sistema.

In questa tesi, il metodo verrà utilizzato per valutare le condizioni di singolarità che possono verificarsi nel sistema durante il suo moto. Una singolarità meccanica è una condizione critica in cui il sistema può iniziare a svolgere un moto diverso dal quello originale. Inoltre, questo approccio viene utilizzato anche per risolvere casi in cui vi sono vincoli ridondanti sul sistema, il che significa che alcuni vincoli non sono indipendenti. In questa tesi sono presentati diversi esempi di meccanismi a quadrilatero articolato e successive modifiche in maniera tale da poter confrontare l'approccio con il minimal coordinate set con e senza algoritmo di continuazione, in modo da valutare quando si verifica una configurazione di singolarità e quando il sistema presenta dei vincoli ridondanti.

Parole chiave: Set minimo di coordinate, fattorizzazione QR, algoritmo di continuazione, configurazione singolarità, vincolo ridondante

Contents

1 | Introduction

1.1. Multibody System Dynamics

The dynamics of multibody systems have emerged as a challenging subject in mechanical systems. This deals with the simulation of movements that occur from bodies, both rigid and flexible, which are connected to each other. The interconnection stems from by kinematic joint and by force element. The motions of this system can be large translational and rotational movements.

There are two basic mechanisms of dynamic multibody systems, namely unconstrained and constrained. An unconstrained system means that the system is not subject to certain kinematic or geometric conditions. Meanwhile, for a constrained system, the movement of the system is limited to certain geometric boundaries. There are several papers that explain an approach to imposing constraints on multibody dynamics systems. For the classic approach, see [10]. While the contemporary approach can be seen in [1].

In a mechanical system, the equations to describe the unconstrained multibody system are usually expressed using ordinary differential equations (ODEs), Eq. (1.1a). Whereas equations to describe the constraint are written in algebraic equations, Eq. (1.1b). Combining those equations leads to the expression of the constrained multibody system dynamics equation. It is commonly called differential-algebraic equations (DAEs).

$$\mathbf{M}(\mathbf{x}, t)\ \ddot{\mathbf{x}} = \mathbf{f}(\mathbf{x}, \dot{\mathbf{x}}, t) \tag{1.1a}$$

$$\mathbf{c}(\mathbf{x}, t) = \mathbf{0} \tag{1.1b}$$

$\mathbf{M} \in \mathbb{R}^{n \times n}$ is the inertial matrix (where it has a possibility to be not constant) with structure symmetric and positive definite. $\mathbf{f} \in \mathbb{R}^n$ is a set of the generalized force, energetically conjugated with the virtual displacement, $\delta\mathbf{x}$. Eq. (1.1) is usually categorized in multibody formulations (based on the literature) into three categories [6]:

1. Minimal Coordinate Set (MCS). This formulation manipulates the equation so that it can be transformed into an ODE problem, reducing the coordinate to a truly

independent one. This approach will be explained in detail in the following section.

2. Redundant Coordinate Set (RCS). In this formulation, the problem is directly solved in DAEs form. It consists of n set coordinates and a set of m Lagrange multipliers.

3. Unconstrained Coordinate Set. The problem is modeled as an unconstrained system with n coordinates then the constraints are added to the formulation. See for example the so-called augmented Lagrangian approach [2] or the force projection method [15], as discussed in [6].

The modification of Eq. (1.1) could be done using Lagrange multipliers, $\boldsymbol{\lambda}$. The multiplication between Lagrange multipliers and the transpose of the constraint Jacobian matrix, $\mathbf{c}_{/\mathbf{x}}$, define the value of the reaction force, $\mathbf{f}_c$.

$$\mathbf{f}_c = \mathbf{c}_{/\mathbf{x}}\boldsymbol{\lambda} \tag{1.2}$$

Therefore, Eq. (1.1a) can be rewritten as

$$\mathbf{M}(\mathbf{x}, t)\ \ddot{\mathbf{x}} + \mathbf{c}_{/\mathbf{x}}^T\boldsymbol{\lambda} = \mathbf{f}(\mathbf{x}, \dot{\mathbf{x}}, t) \tag{1.3}$$

1.2. Minimal Coordinate Set

Using the minimal coordinate set approach, matrix $\mathbf{T}$ needs to be suitably defined. Considering a system with n ordinary differential equations greater than m number of constraints and the constraint Jacobian matrix is full rank, the size of matrix $\mathbf{T}$ is $\mathbb{R}^{n\times(n-m)}$. This matrix is obtained by the following definition:

$$\dot{\mathbf{x}} = \mathbf{T}\dot{\mathbf{q}} + \beta' \tag{1.4a}$$

$$\ddot{\mathbf{x}} = \mathbf{T}\ddot{\mathbf{q}} + \beta'' \tag{1.4b}$$

where $\mathbf{x} \in \mathbb{R}^n$ is a physical coordinates and $\mathbf{q} \in \mathbb{R}^{n-m}$ is a generalized coordinates which is local and independent. Besides that, β' and β'' are defined through the time derivative of the constraint equations, Eq. (1.1b). The detailed derivation could be seen in [23]. The result is displayed in the following equations where $\mathbf{c}_{/\mathbf{x}} \in \mathbb{R}^{m\times n}$ is the constraint Jacobian matrix.

$$\mathbf{c}_{/\mathbf{x}}\beta' = -\mathbf{c}_{/t} \tag{1.5a}$$

$$\mathbf{c}_{/\mathbf{x}}\beta'' = -(\dot{\mathbf{c}})_{/\mathbf{x}} - (\dot{\mathbf{c}})_{/t} \tag{1.5b}$$

Substituting Eq. (1.4b) to Eq. (1.3), leads to the equation of the constrained system dynamics become:

$$\mathbf{T}^T\mathbf{M}\mathbf{T}\ddot{\mathbf{q}} + \cancel{\mathbf{T}^T\mathbf{A}^T}\lambda = \mathbf{T}^T(\mathbf{f} - \mathbf{M}\beta'') \tag{1.6}$$

Matrix $\mathbf{T}$ describes a space spanned by coordinate $\mathbf{x}$ and tangent to constraint manifold. Whereas, matrix $\mathbf{A} \equiv \mathbf{c}_{/\mathbf{x}}$ is the constraint Jacobian matrix. The matrix can have the relation $\mathbf{T}^T\mathbf{A}^T \equiv \mathbf{0} \in \mathbb{R}^{(n-m)\times m}$ if the constraints are assumed to be ideal. If the constraint is not ideal, for example, the presence of friction, the term $\mathbf{T}^T\mathbf{A}^T$ can not be canceled. In this case, The Lagrange multiplier is required and is calculated from the local equilibria.

2 | QR and QRP Factorization

2.1. QR Factorization

This thesis focuses on using QR factorization to find the suitable matrix $\mathbf{T}$ needed in the MCS approach. Other approaches could be used such as the ones proposed in [14]: e.g., coordinate partitioning [7, 20], zero eigenvalues [18], singular value decomposition; [13, 19], and QR factorization [5], etc.

Considering a system with $n > m$ and matrix $\mathbf{A}$ is full rank. Matrix $\mathbf{T}$ is defined as follows:

$$\mathbf{A}^T = \mathbf{QR} = [\mathbf{Q}_1 \ \mathbf{Q}_2] \begin{bmatrix} \mathbf{R}_1 \\ \mathbf{0} \end{bmatrix} = \mathbf{Q}_1 \mathbf{R}_1 \tag{2.1}$$

with $\mathbf{A} \in \mathbb{R}^{m \times n}$, $\mathbf{Q}_1 \in \mathbb{R}^{n \times m}$, $\mathbf{Q}_2 \in \mathbb{R}^{n \times (n-m)}$, $\mathbf{R}_1 \in \mathbb{R}^{m \times m}$. Matrix $\mathbf{Q}_2$ is defined as the suitable matrix $\mathbf{T}$. Therefore, Eq. (1.4a) and Eq. (1.4b) can be written as

$$\dot{\mathbf{x}} = \mathbf{Q}_2 \dot{\mathbf{q}} + \mathbf{Q}_1 \mathbf{p}' \tag{2.2a}$$
$$\ddot{\mathbf{x}} = \mathbf{Q}_2 \ddot{\mathbf{q}} + \mathbf{Q}_1 \mathbf{p}'' \tag{2.2b}$$

Using definition $\beta' = \mathbf{Q}_1 \mathbf{p}'$ and $\beta'' = \mathbf{Q}_1 \mathbf{p}''$, Eq. (1.5a) and Eq. (1.5b) could be modified as (the detail modification can be seen in [23]):

$$\mathbf{p}' = -\mathbf{R}_1^{-T} \mathbf{c}_{/t} \tag{2.3a}$$
$$\mathbf{p}'' = -\mathbf{R}_1^{-T} [(\dot{\mathbf{c}})_{/\mathbf{x}} \dot{\mathbf{x}} - (\dot{\mathbf{c}})_{/t}] \tag{2.3b}$$

In the end, the equation of the constrained multibody systems could be written as

$$\begin{aligned} \mathbf{T}^T \mathbf{M} \mathbf{T} \ddot{\mathbf{q}} &= \mathbf{T}^T (\mathbf{f} - \mathbf{M} \beta'') \\ \dot{\mathbf{x}} &= \mathbf{T} \dot{\mathbf{q}} + \mathbf{Q}_1 \mathbf{p}' \end{aligned} \tag{2.4}$$

The form (Eq. 2.4) was originally constructed by Maggi [11, 12] and later re-proposed by Kane [9], is now often called the Maggi-Kane [3] equation.

The previously mentioned form contains ordinary differential equations (ODEs) with physical coordinates, $\mathbf{x}$, and generalized coordinates, $\mathbf{q}$, as unknown variables. Therefore it is easy to be integrated. Integrating that equation yields velocity in the generalized coordinates, $\dot{\mathbf{q}}$ and position in the physical coordinates, $\mathbf{x}$. Then, using a simple equation in Eq. (2.2a), it is easy to find the physical velocities, $\dot{\mathbf{x}}$.

The obtained physical coordinates needs to be corrected. Because the result of the integration of the constraint derivative might make the set of unconstrained coordinates not satisfy the constraint manifold. The correction is done by taking a linearization of constraint equations.

$$\mathbf{c}(\mathbf{x}, t) = \mathbf{c}\left(\mathbf{x}^{(0)}, t\right) + \mathbf{c}_{/\mathbf{x}}\Big|_{\mathbf{x}^{(0)}} \Delta\mathbf{x} = \mathbf{0} \tag{2.5}$$

A solution is sought in the form,

$$\Delta\mathbf{x} = \mathbf{Q}_1\Delta\boldsymbol{\nu} + \mathbf{Q}_2\Delta\boldsymbol{\psi} \tag{2.6}$$

Considering the ideal constraint, the equation can be rewritten as

$$\begin{aligned} \mathbf{c}\left(\mathbf{x}^{(0)}, t\right) + \mathbf{c}_{/\mathbf{x}}\Big|_{\mathbf{x}^{(0)}} \Delta\mathbf{x} &= \mathbf{c}\left(\mathbf{x}^{(0)}, t\right) + \mathbf{A}(\mathbf{Q}_1\Delta\boldsymbol{\nu} + \mathbf{Q}_2\Delta\boldsymbol{\psi}) \\ &= \mathbf{c}\left(\mathbf{x}^{(0)}, t\right) + \mathbf{A}\mathbf{Q}_1\Delta\boldsymbol{\nu} + \cancel{\mathbf{A}\mathbf{T}}\Delta\boldsymbol{\psi} = \mathbf{0} \end{aligned} \tag{2.7}$$

so that,

$$\Delta\boldsymbol{\nu} = -(\mathbf{A}\mathbf{Q}_1)^{-1}\mathbf{c}\left(\mathbf{x}^{(0)}, t\right) \tag{2.8}$$

The solution is updated as

$$\mathbf{x}^{(1)} = \mathbf{x}^{(0)} + \mathbf{Q}_1\Delta\boldsymbol{\nu} \tag{2.9}$$

The process is repeated until convergence. For each iteration, matrix $\mathbf{c}_{/\mathbf{x}}$ may depend on $\mathbf{x}$, so it should be updated while iterating using QR factorization. The formula can be written as

$$\mathbf{x}^{(i+1)} = \mathbf{x}^{(i)} - \mathbf{Q}_1(\mathbf{A}\mathbf{Q}_1)^{-1}\mathbf{c}\left(\mathbf{x}^{(i)}, t\right) \tag{2.10}$$

$(.)^{(i)}$ is the estimation of the value at i-th itteration.

Besides that, the velocity ($\dot{\mathbf{x}}$) needs to be corrected to comply with the derivative of constraint, namely $\mathbf{c}_{/\mathbf{x}}\dot{\mathbf{x}} = 0$. The formula can be seen as follows,

$$\dot{\mathbf{x}} = \mathbf{T}^T\mathbf{T}\dot{\mathbf{x}} \tag{2.11}$$

2.2. QRP for Singularity

If the system experiences a singularity configuration during its motion, some care of the solution process needs to be taken into account. The singularity configuration is a critical condition in which the system has the possibility to choose another movement that may be very different from the original movement during its motion. Numerically, it can be observed by checking the rank of matrix $\mathbf{A}$. If the rank of matrix $\mathbf{A}$ reduces (some of its rows are not linearly independent), the degree of freedom of the system will increase, and the system experiences another movement. In this case, the definition of the suitable matrix $\mathbf{T}$ needs to be updated. The QR factorization also needs to be redefined in the sense that the diagonal of matrix $\mathbf{R}$ is arranged in decreased order of their norm. It could be done by introducing a permutation matrix, $\mathbf{P}$ [8], so the Eq. (2.1) could be written as:

$$\mathbf{A}^T = \mathbf{Q}\mathbf{R}\mathbf{P}^T \tag{2.12}$$

Decomposing matrix $\mathbf{Q}$ and $\mathbf{R}$ as seen in Eq. 2.1

$$\mathbf{A}^T = \begin{bmatrix}\mathbf{Q}_1 & \mathbf{Q}_2\end{bmatrix}\begin{bmatrix}\mathbf{R}_1 \\ \mathbf{0}\end{bmatrix}\mathbf{P}^T \tag{2.13}$$

and when the singularity condition occurs, Eq. 2.12 can be written as

$$\mathbf{A}^T = \begin{bmatrix}\begin{bmatrix}\mathbf{Q}_{1\text{ns}} & \mathbf{Q}_{1\text{s}}\end{bmatrix}\mathbf{Q}_2\end{bmatrix}\begin{bmatrix}\begin{bmatrix}\mathbf{R}_{1\text{ns}} & \mathbf{R}_{1\text{s}} \\ \cdots & \mathbf{0}\end{bmatrix} \\ \mathbf{0}\end{bmatrix}\mathbf{P}^T \tag{2.14}$$

with $\mathbf{Q}_{1\text{ns}} \in \mathbb{R}^{n\times(m-d)}$, $\mathbf{Q}_{1\text{s}} \in \mathbb{R}^{n\times d}$, $\mathbf{Q}_2 \in \mathbb{R}^{n\times(n-m)}$, $\mathbf{R}_{1_{ns}} \in \mathbb{R}^{(m-d)\times(m-d)}$, and $\mathbf{R}_{1_s} \in \mathbb{R}^{(m-d)\times d}$. d is the number of deficiency ranks of the constraint Jacobian matrix. It can be obtained from the difference between the lesser of the number of rows and columns of matrix $\mathbf{A}$ and the rank of that matrix, such that $d = m - \text{rank}(\mathbf{A})$. It explains that when a rank deficiency occurs, some constraints are become redundant, meaning they are not independent anymore. Thus, the rank of matrix $\mathbf{A}$ decreases. The number by which the rank reduces indicates the number of increased degrees of freedom in the system. For example, when a system is moving, and at some point, the rank of matrix $\mathbf{A}$ suddenly experiences a reduction (assuming one reduction, $d = 1$). At that moment, the system experiences one additional degree of freedom, because one constraint becomes redundant. Some examples of mechanisms and their evaluation are presented in this thesis when the singularity occurs.

The equation of constrained multibody systems still has the same structure as Eq. (2.4) but with an updated suitable subspace matrix $\mathbf{T}$. Matrix $\mathbf{T}$ is written as follows,

$$\mathbf{T} = \begin{bmatrix} \mathbf{Q}_{1\text{s}} & \mathbf{Q}_2 \end{bmatrix} \tag{2.15}$$

Now matrix $\mathbf{T}$ has dimension $\mathbf{T} \in \mathbb{R}^{n\times(n-m+d)}$.

3 | Continuation Algorithm

The purpose of the continuation method is to preserve some sort of spatial continuity of generalized coordinate, $\mathbf{q}$. This is done by minimizing the deviation of subspace that intrinsically needs to maintain $\mathbf{Q}_2$ tangent to constraint manifold along the time. To make it understandable-see this illustration.

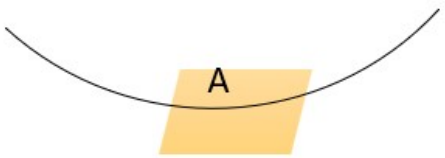

(a) Solution subspace

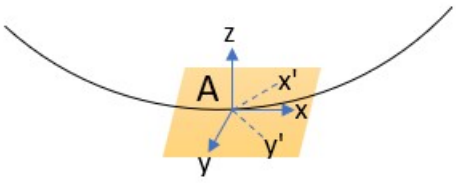

(b) Selected solution subspace

Figure 3.1: Subspace selection and continuation process description

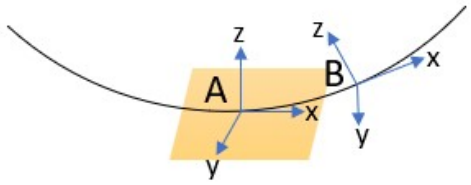

(c) Continuation of selected solution subspace

Figure 3.1: Subspace selection and continuation process description

The yellow space is the space tangent to the constraint manifold, where an infinite possible subspace of matrix $\mathbf{Q}_2$ could be selected as shown in Fig. 3.1a. Using QR Factorization, vector-matrix $\mathbf{Q}_2$ will be picked randomly (see vectors $x - y$ and $x' - y'$ in Fig. 3.1b, assuming the selected subspace in this point is in vector $x - y$). Without continuation, the selected subspace after integration can not be controlled, meaning the next subspace may have a different orientation than the previous one. Whereas with continuation, the subspace selection can be handled to be as close as possible to the previous subspace. As shown in Fig. 3.1c, point B represents the point after integration, and the subspace of $\mathbf{Q}_2$ at that point is chosen in such a way as to be close to the subspace before integration (point A).

The continuation for a system with $m < n$ and having the total rank of matrix $\mathbf{A}$ is done by Zhou, *et al.* and can be seen in [23]. Meanwhile, the implementation of the continuation approach with a system that has redundant constraints will be explained in the next chapter.

4 Redundant Constraint

4.1. Rank-Deficient Constraint Jacobian Matrix

4.1.1. Traditional QR

Consider the system with $m < n$ and the rank of matrix $\mathbf{A}$ is not full-rank, meaning the matrix has a rank deficiency, d. The suitable subspace can be chosen using QR factorization with permutation [16]. This approach has been explained in Section 2.2 when dealing with singularity. The following shows the calculation of the $\mathbf{A}$ matrix for completeness.

$$\begin{aligned}\mathbf{A}^T &= \begin{bmatrix}\mathbf{Q}_1 & \mathbf{Q}_2\end{bmatrix}\begin{bmatrix}\mathbf{R}_1 \\ \mathbf{0}\end{bmatrix}\mathbf{P}^T \\ &= \left[\begin{bmatrix}\mathbf{Q}_{1\text{ns}} & \mathbf{Q}_{1\text{s}}\end{bmatrix}\mathbf{Q}_2\right]\begin{bmatrix}\begin{bmatrix}\mathbf{R}_{1\text{ns}} & \mathbf{R}_{1\text{s}} \\ \cdots & \mathbf{0}\end{bmatrix} \\ \mathbf{0}\end{bmatrix}\mathbf{P}^T\end{aligned} \tag{4.1}$$

In this problem, the definition of the suitable matrix $\mathbf{T}$ consists of $\mathbf{Q}_{1_s}$ and $\mathbf{Q}_2$. Thus, matrix $\mathbf{T}$ has dimension $\mathbf{T} \in \mathbb{R}^{n\times(n-m+d)}$, the formula can be seen in Eq. (4.2)

$$\mathbf{T} = \begin{bmatrix}\mathbf{Q}_{1\text{s}} & \mathbf{Q}_2\end{bmatrix} \tag{4.2}$$

Besides that, if the system has the same number of ordinary differential equations and constraints ($n = m$), and there is a redundancy in the constraint Jacobian matrix (matrix $\mathbf{A}$ is not full rank), the definition of the suitable matrix $\mathbf{T}$ only consists of $\mathbf{Q}_{1_s}$ alone, because matrix $\mathbf{Q}_2$ is empty. The suitable matrix $\mathbf{T}$ has dimension $\mathbf{T} \in \mathbb{R}^{n\times d}$ and is defined as:

$$\mathbf{T} = \mathbf{Q}_{1_s} \tag{4.3}$$

4.1.2. Continuation Algorithm

As explained in Chapter 3 about the purpose of this algorithm, with a slight adjustment, the continuation algorithm can also be applied to this case, the system with $m \leq n$ and $d > 0$. First, taking the time derivative of matrix $\mathbf{A}$

$$\dot{\mathbf{A}}^T = \dot{\mathbf{Q}}\mathbf{R}\mathbf{P}^T + \mathbf{Q}\dot{\mathbf{R}}\mathbf{P}^T = \begin{bmatrix}\dot{\mathbf{Q}}_1 & \dot{\mathbf{Q}}_2\end{bmatrix}\begin{bmatrix}\mathbf{R}_1 \\ \mathbf{0}\end{bmatrix}\mathbf{P}^T + \begin{bmatrix}\mathbf{Q}_1 & \mathbf{Q}_2\end{bmatrix}\begin{bmatrix}\dot{\mathbf{R}}_1 \\ \mathbf{0}\end{bmatrix}\mathbf{P}^T \tag{4.4}$$

Then, pre-multiply Eq. (4.4) with matrix $\mathbf{Q}^T$ and post-multiply it by matrix $\mathbf{P}$, and also exploiting the orthogonality, the equation will be

$$\mathbf{Q}^T\dot{\mathbf{A}}^T\mathbf{P} = \mathbf{Q}^T\dot{\mathbf{Q}}\mathbf{R} + \dot{\mathbf{R}} \tag{4.5}$$

Using the definition of

$$\mathbf{Q}^T\dot{\mathbf{Q}} = \mathbf{\Omega} = -\mathbf{\Omega}^T \tag{4.6}$$

with $\mathbf{\Omega} \in \mathbb{R}^{n\times n}$, because of the orthogonality of matrix $\mathbf{Q}$. Back to the Eq. (4.5) and define as

$$\mathbf{Q}^T\dot{\mathbf{A}}^T\mathbf{P} = \mathbf{J} \tag{4.7}$$

Then, Eq. (4.5) can be rewritten by considering non-singular 'ns' and singular 's' blocks, namely:

$$\begin{bmatrix}\mathbf{J}_{11} & \mathbf{J}_{12} \\ \mathbf{J}_{21} & \mathbf{J}_{22}\end{bmatrix} = \begin{bmatrix}\mathbf{\Omega}_{ns} & -\mathbf{\Omega}_s^T \\ \mathbf{\Omega}_s & \mathbf{0}\end{bmatrix}\begin{bmatrix}\mathbf{R}_{1_{ns}} & \mathbf{R}_{1_s} \\ \mathbf{0} & \mathbf{0}\end{bmatrix} + \begin{bmatrix}\dot{\mathbf{R}}_{1_{ns}} & \dot{\mathbf{R}}_{1_s} \\ \mathbf{0} & \mathbf{0}\end{bmatrix} \tag{4.8}$$

with $\mathbf{J}_{11} \in \mathbb{R}^{(m-d)\times(m-d)}$, $\mathbf{J}_{12} \in \mathbb{R}^{(m-d)\times d}$, $\mathbf{J}_{21} \in \mathbb{R}^{(n-m+d)\times(m-d)}$, $\mathbf{J}_{22} \in \mathbb{R}^{(n-m+d)\times d}$, $\mathbf{\Omega}_{ns} \in \mathbb{R}^{(m-d)\times(m-d)}$, $\mathbf{\Omega}_s \in \mathbb{R}^{(n-m+d)\times(m-d)}$, $\mathbf{R}_{1_{ns}} \in \mathbb{R}^{(m-d)\times(m-d)}$, and $\mathbf{R}_{1_s} \in \mathbb{R}^{(m-d)\times d}$. The bottom-right of matrix $\mathbf{\Omega}$ is set to be zero to minimize the re-orientation of the vector of the suitable matrix $\mathbf{T}$ that corresponds to the direction of motion allowed by rank deficiency of the constraint Jacobian matrix, $\mathbf{A}$. Eq. (4.8) can be expressed by four equations as follows:

$$\mathbf{J}_{11} = \boldsymbol{\Omega}_{ns}\mathbf{R}_{1_{ns}} + \dot{\mathbf{R}}_{1_{ns}} \tag{4.9a}$$

$$\mathbf{J}_{12} = \boldsymbol{\Omega}_{ns}\mathbf{R}_{1_{s}} + \dot{\mathbf{R}}_{1_{s}} \tag{4.9b}$$

$$\mathbf{J}_{21} = \boldsymbol{\Omega}_{s}\mathbf{R}_{1_{ns}} \tag{4.9c}$$

$$\mathbf{J}_{22} = \boldsymbol{\Omega}_{s}\mathbf{R}_{1_{s}} \tag{4.9d}$$

From Eq. (4.9c), it can be rewritten as

$$\boldsymbol{\Omega}_{s} = \mathbf{J}_{21}\mathbf{R}_{1_{ns}}^{-1} \tag{4.10}$$

From Eq. (4.9a) do a manipulation of by post-multiplication with $\mathbf{R}_{1_{ns}}^{-1}$.

$$\mathbf{J}_{11}\mathbf{R}_{1_{ns}}^{-1} = \boldsymbol{\Omega}_{ns} + \dot{\mathbf{R}}_{1_{ns}}\mathbf{R}_{1_{ns}}^{-1} \tag{4.11}$$

Then, consider its strictly lower triangular part (remember that matrix $\mathbf{R}_{1_{ns}}$ and its derivative are upper triangular matrix), the equation will be

$$\text{stril}(\mathbf{J}_{11}\mathbf{R}_{1_{ns}}^{-1}) = \text{stril}(\boldsymbol{\Omega}_{ns}) + \text{stril}(\cancel{\dot{\mathbf{R}}_{1_{ns}}\mathbf{R}_{1_{ns}}^{-1}}) = \boldsymbol{\Omega}_{L} \tag{4.12}$$

So that,

$$\boldsymbol{\Omega}_{ns} = \boldsymbol{\Omega}_{L} - \boldsymbol{\Omega}^{T} \tag{4.13}$$

Thus, $\boldsymbol{\Omega}$ can be arranged according to Eq. (4.8) by filling in the non-singular and singular blocks. Based on Eq. (4.6), matrix $\mathbf{Q}$ for continuation can be obtained by integrating these equations. Integration must be carried out with appropriate steps by considering the integration results (matrix $\mathbf{Q}$) must maintain the orthogonality and the submatrix $\mathbf{Q}_1$ matches with the one resulting from the factorization of the transpose of the constraint Jacobian matrix (e.g., using the Munthe-Kaas method [17]).

Assuming constant $\boldsymbol{\Omega}$, the integration from time t_k to t_{k+1} of matrix $\mathbf{Q}$ can be seen as follows

$$\mathbf{Q}_{t_{k+1}} = \mathbf{Q}_{t_k}\mathrm{e}^{\boldsymbol{\Omega}h} \tag{4.14}$$

After getting matrix $\mathbf{Q}$, it is necessary to reorthogonalize the suitable matrix because

the solutions of the continuation and QR factorization may differ. This is due to the accumulation of numerical errors during integration. The reorthogonalization can be seen in Appendix A.

4.2. Constraints Exceeding the Number of Coordinates

4.2.1. Traditional QR

Considering the system with $m > n$ and has some redundant constraints, which means the constrained Jacobian matrix of this system is not full-rank. d is the number of admissible motions of the system. d can be computed using the difference between the lesser number of rows or columns of matrix $\mathbf{A}$ and the rank of that matrix itself, such that $d = n - \text{rank}\mathbf{A}$.

Furthermore, using the QRP factorization of matrix $\mathbf{A}^T$ [16], the results is

$$\mathbf{A}^T = \mathbf{Q}\mathbf{R}\mathbf{P}^T = \mathbf{Q}_1 \begin{bmatrix} \mathbf{R}_1 & \mathbf{R}_2 \end{bmatrix} \mathbf{P}^T \tag{4.15}$$

with $\mathbf{Q}_1 \in \mathbb{R}^{n\times n}$, $\mathbf{R}_1 \in \mathbb{R}^{n\times n}$, $\mathbf{R}_2 \in \mathbb{R}^{n\times(n-m)}$, and $\mathbf{P} \in \mathbb{R}^{m\times m}$. In this system, matrix $\mathbf{Q}$ does not have component $\mathbf{Q}_2$. Instead, matrix $\mathbf{R}$ have component $\mathbf{R}_2$.

Considering the non-singular 'ns' and singular 's' block, Eq. 4.15 can be rearranged to

$$\mathbf{A}^T = \begin{bmatrix} \mathbf{Q}_{1\text{ns}} & \mathbf{Q}_{1\text{s}} \end{bmatrix} \begin{bmatrix} \begin{bmatrix} \mathbf{R}_{1\text{ns}} & \mathbf{R}_{1\text{s}} \\ \cdots & \mathbf{0} \end{bmatrix} \mathbf{R}_2 \end{bmatrix} \mathbf{P}^T \tag{4.16}$$

with $\mathbf{Q}_{1\text{ns}} \in \mathbb{R}^{n\times(n-d)}$, $\mathbf{Q}_{1\text{s}} \in \mathbb{R}^{n\times d}$, $\mathbf{R}_{1\text{ns}} \in \mathbb{R}^{(n-d)\times(n-d)}$, $\mathbf{R}_{1\text{s}} \in \mathbb{R}^{(n-d)\times d}$, and $\mathbf{R}_2 \in \mathbb{R}^{n\times(m-n)}$. Therefore the suitable subspace $\mathbf{T} \in \mathbb{R}^{n\times d}$ is defined as

$$\mathbf{T} = \mathbf{Q}_{1\text{s}} \tag{4.17}$$

4.2.2. Continuation Algorithm

The procedure is the same as the continuation in Section 4.1. However, there are small differences that must be considered. Consider the time derivative of constraint Jacobian matrix, $\mathbf{A}$.

$$\dot{\mathbf{A}}^T = \dot{\mathbf{Q}}_1\mathbf{R}\mathbf{P}^T + \mathbf{Q}_1\dot{\mathbf{R}}\mathbf{P}^T = \dot{\mathbf{Q}}_1\begin{bmatrix}\mathbf{R}_1 & \mathbf{R}_2\end{bmatrix}\mathbf{P}^T + \mathbf{Q}_1\begin{bmatrix}\dot{\mathbf{R}}_1 & \dot{\mathbf{R}}_2\end{bmatrix}\mathbf{P}^T \tag{4.18}$$

Then do a pre-multiplication with $\mathbf{Q}_1^T$ and post-multiplication with $\mathbf{P}$. Exploiting the orthogonality of the matrix. The equation will be

$$\mathbf{Q}_1^T\dot{\mathbf{A}}^T\mathbf{P} = \mathbf{Q}_1^T\dot{\mathbf{Q}}_1\begin{bmatrix}\mathbf{R}_1 & \mathbf{R}_2\end{bmatrix} + \begin{bmatrix}\dot{\mathbf{R}}_1 & \dot{\mathbf{R}}_2\end{bmatrix} \tag{4.19}$$

The $\mathbf{\Omega}$ is defined as

$$\mathbf{Q}_1^T\dot{\mathbf{Q}}_1 = \mathbf{\Omega} = -\mathbf{\Omega}^T \tag{4.20}$$

by exploiting the orthogonality of matrix $\mathbf{Q}_1$, the dimension of $\mathbf{\Omega}$ is $\mathbf{\Omega} \in \mathbb{R}^{n\times n}$.

Considering the first n columns of both sides of Eq. (4.19), and called as $\mathbf{J}$

$$\mathbf{Q}_1^T\dot{\mathbf{A}}^T\mathbf{P}(:, 1:n) = \mathbf{J} \tag{4.21}$$

Then, split the matrix with block non-singular 'ns' and singular 's' so that the equation will become

$$\begin{bmatrix}\mathbf{J}_{11} & \mathbf{J}_{12}\\ \mathbf{J}_{21} & \mathbf{J}_{22}\end{bmatrix} = \begin{bmatrix}\mathbf{\Omega}_{ns} & -\mathbf{\Omega}_s^T\\ \mathbf{\Omega}_s & \mathbf{0}\end{bmatrix}\begin{bmatrix}\mathbf{R}_{1_{ns}} & \mathbf{R}_{1_s}\\ \mathbf{0} & \mathbf{0}\end{bmatrix} + \begin{bmatrix}\dot{\mathbf{R}}_{1_{ns}} & \dot{\mathbf{R}}_{1_s}\\ \mathbf{0} & \mathbf{0}\end{bmatrix} \tag{4.22}$$

From there, four equations are developed as follows,

$$\mathbf{J}_{11} = \mathbf{\Omega}_{ns}\mathbf{R}_{1_{ns}} + \dot{\mathbf{R}}_{1_{ns}} \tag{4.23a}$$
$$\mathbf{J}_{12} = \mathbf{\Omega}_{ns}\mathbf{R}_{1_s} + \dot{\mathbf{R}}_{1_s} \tag{4.23b}$$
$$\mathbf{J}_{21} = \mathbf{\Omega}_s\mathbf{R}_{1_{ns}} \tag{4.23c}$$
$$\mathbf{J}_{22} = \mathbf{\Omega}_s\mathbf{R}_{1_s} \tag{4.23d}$$

From Eq. (4.23c)

$$\mathbf{\Omega}_s = \mathbf{J}_{21}\mathbf{R}_{1_{ns}}^{-1} \tag{4.24}$$

Then, from Eq. (4.23a), do the post-multiplication with $\mathbf{R}_{1_{ns}}^{-1}$

$$\mathbf{J}_{11}\mathbf{R}_{1_{ns}}^{-1} = \mathbf{\Omega}_{ns} + \dot{\mathbf{R}}_{1_{ns}}\mathbf{R}_{1_{ns}}^{-1} \tag{4.25}$$

Remember that matrix $\mathbf{R}_{1_{ns}}$ and its derivative is upper triangular matrices, so by considering a strictly lower triangular part of Eq. (4.25), it will obtain

$$\text{stril}(\mathbf{J}_{11}\mathbf{R}_{1_{ns}}^{-1}) = \text{stril}(\mathbf{\Omega}_{ns}) + \text{stril}(\cancel{\dot{\mathbf{R}}_{1_{ns}}\mathbf{R}_{1_{ns}}^{-1}}) = \mathbf{\Omega}_L \tag{4.26}$$

So that,

$$\mathbf{\Omega}_{ns} = \mathbf{\Omega}_L - \mathbf{\Omega}_L^T \tag{4.27}$$

Compiling matrix $\mathbf{\Omega}$ and integrating Eq. (4.20) from time t_k to time t_{k+1}, will obtain matrix $\mathbf{Q}$ from continuation. The integration must be done with proper steps to maintain the orthogonality of the result of $\mathbf{Q}$ and to guarantee $\mathbf{Q}_1$ is the same as when using factorization.

$$\mathbf{Q}_{t_{k+1}} = \mathbf{Q}_{t_k}\mathrm{e}^{\mathbf{\Omega}h} \tag{4.28}$$

It is necessary to do a reorthogonalization of the result because the solution from QR factorization and continuation may differ due to the accumulation of numerical error during the integration. The reorthogonalization can be seen in Appendix A.

5 | Results and Analysis

5.1. Spatial Pendulum

Consider a multi-degree of freedom of spatial pendulum with mass $M = 1$ kg and length $\ell = 0.08$ m. This system is adapted from the original problem in [23]. The analysis of the results obtained from this model will allow for choosing a proper time step (h) to be implemented, which will be used in the simulation of all the systems covered in this thesis.

The initial position and velocity, in this case, are $\mathbf{r}_0 = [\ell, 0, 0]^T$ and $\mathbf{v}_0 = [0, 0.7895, 0]^T$. Due to gravity ($\mathbf{g} = 9.81\,\mathrm{m/s^2}$), the pendulum will experience an external force that always points out downward.

The constraint dynamics equation of the spatial pendulum can be seen in Equation 5.1.

$$\begin{bmatrix} M & 0 & 0 \\ 0 & M & 0 \\ 0 & 0 & M \end{bmatrix} \begin{Bmatrix} \ddot{x} \\ \ddot{y} \\ \ddot{z} \end{Bmatrix} + \begin{bmatrix} 2x \\ 2y \\ 2z \end{bmatrix} = \begin{Bmatrix} 0 \\ 0 \\ -Mg \end{Bmatrix} \tag{5.1}$$

with constraint

$$\mathrm{x}^2 + \mathrm{y}^2 + \mathrm{z}^2 + \ell^2 = 0 \tag{5.2}$$

Based on Eq. 5.2, the type of the constraint is time-independent, called `scleronomic` constraint. The jacobian matrix is obtained through the partial derivative of the constraint with respect to the coordinates.

$$\mathbf{A} = [2\mathrm{x}\ 2\mathrm{y}\ 2\mathrm{z}] \tag{5.3}$$

Then, the suitable matrix $\mathbf{T}$ is obtained from the QR factorization using Matlab through a `qr` function. Finally, the equation will become the ordinary differential equations (ODEs)

as shown in Eq. (2.4). This equation can be easily solved by integration. The integration is performed using explicit Runge-Kutta scheme [4] and implemented in Matlab using ode45 with Real tolerance and Absolute tolerance equal to 10^{-6}.

Fig. 5.1 displays the comparison of the time history of the pendulum's position with different time steps (h).

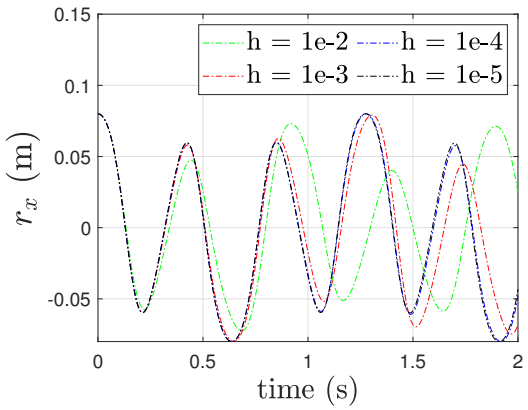

(a) The position of the pendulum in the x direction

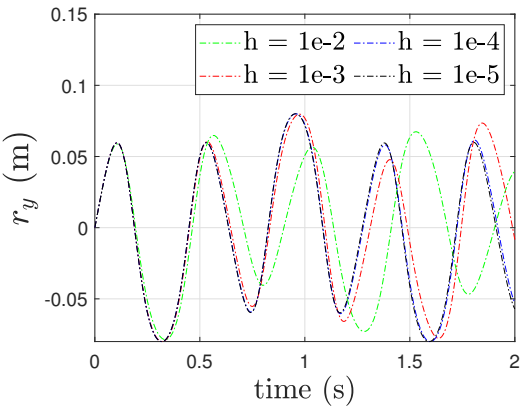

(b) The position of the pendulum in the y direction

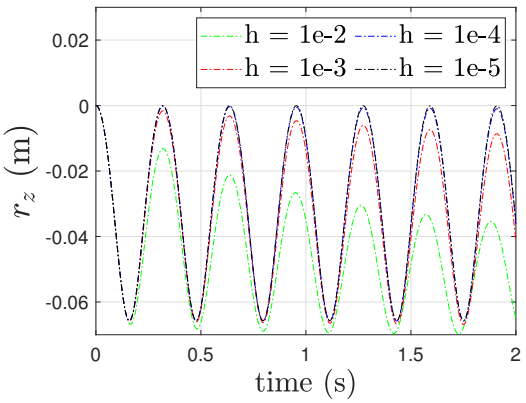

(c) The position of the pendulum in the z direction

Figure 5.1: The time history of position of the spatial pendulum

Moreover, Fig. 5.2 shows the velocity comparison also with different time steps (h).

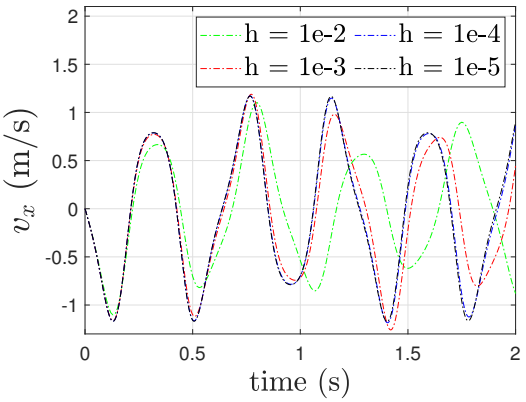

(a) The pendulum's velocity in the x direction

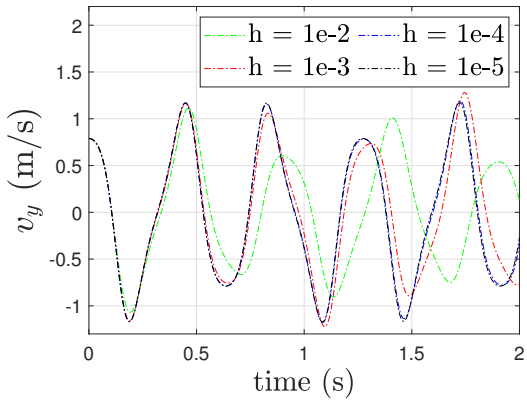

(b) The pendulum's velocity in the y direction

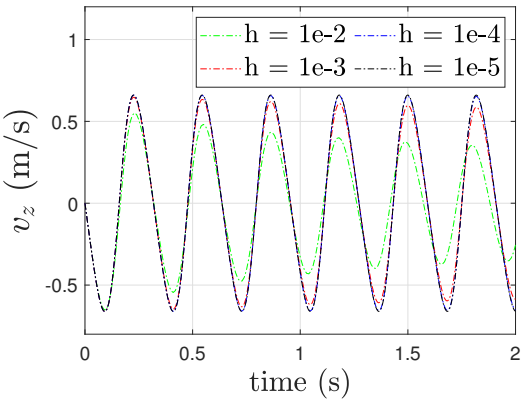

(c) The pendulum's velocity in the z direction

Figure 5.2: The velocity's time history of the spatial pendulum

Based on the results of the time history of the position and velocity comparison, the time history of time steps (h) 10^{-4} seconds and 10^{-5} seconds is quite similar, meaning that the simulation with a time step of 10^{-4} seconds is good enough. Therefore, the rest of the simulation will use the time step h = 10^{-4} seconds to reduce simulation cost.

Furthermore, Figure 5.3 shows the plot of matrix $\mathbf{R}_1$ after sorting the diagonal value to be decreasing order of their norm.

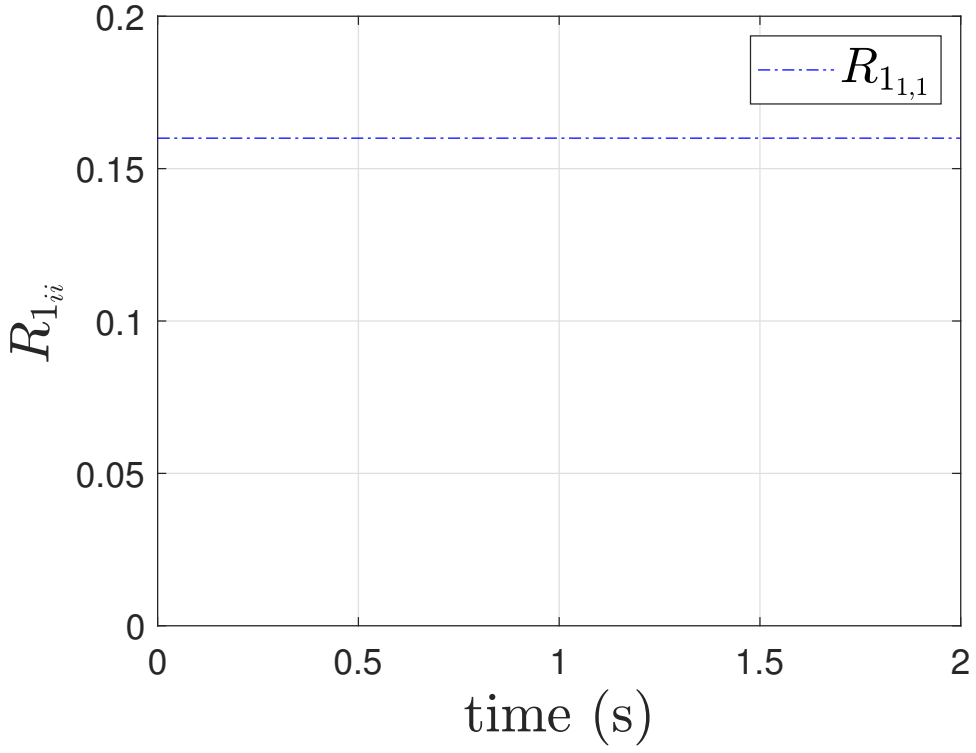

Figure 5.3: The time history of the diagonal coefficient of R_1 of the spatial pendulum

5.1.1. Continuation Algorithm for Spatial Pendulum

Consider the previous spatial pendulum model. In this part, the continuation algorithm is applied to maintain the continuity of the generalized coordinates, $\mathbf{q}$, by tracking the evolution of a suitable matrix $\mathbf{T}$. The result of the time history of $\mathbf{q}$ can be seen in Figure 5.4.

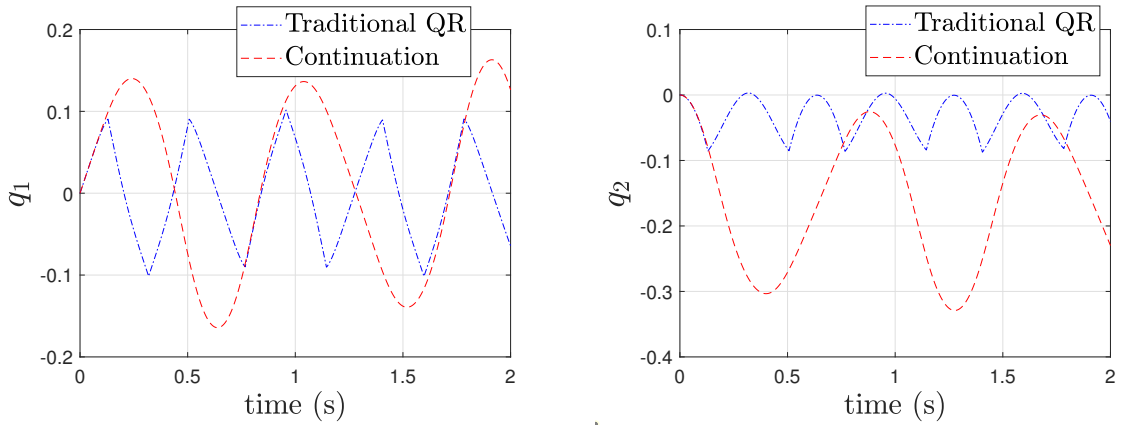

(a) The time history of q_1 (b) The time history of q_2

Figure 5.4: Time history of the generalized coordinates of the spatial pendulum

Besides that, the time history of projected generalized velocities can be observed in Fig. 5.5

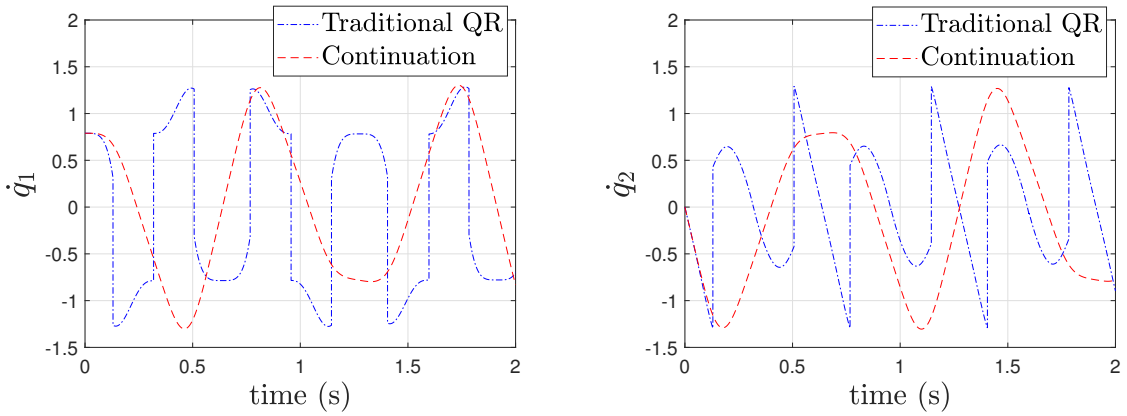

(a) The time history of $\dot{q}_1$ (b) The time history of $\dot{q}_2$

Figure 5.5: Time history of the projected velocities of the spatial pendulum

Using a continuation algorithm produces the values $\mathbf{q}$ that are continuous over time, with no jump in values like what is displayed when using a traditional QR. Furthermore, the figures below show the comparison of physical coordinates (r_x, r_y, and r_z) using traditional and continuation algorithm. It can be seen that adding continuity does not change the results of the physical coordinates (compared to traditional QR), meaning that using the continuation will only affect the generalized coordinates to make them continuous.

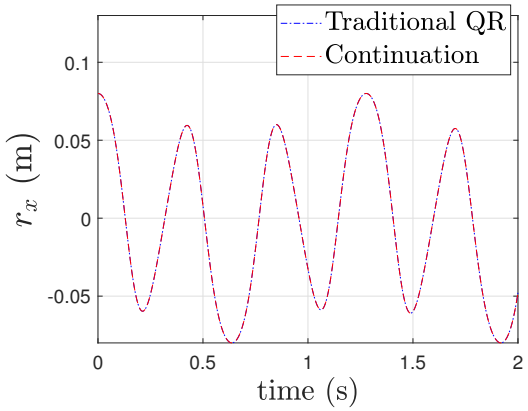

(a) The position of pendulum in x direction

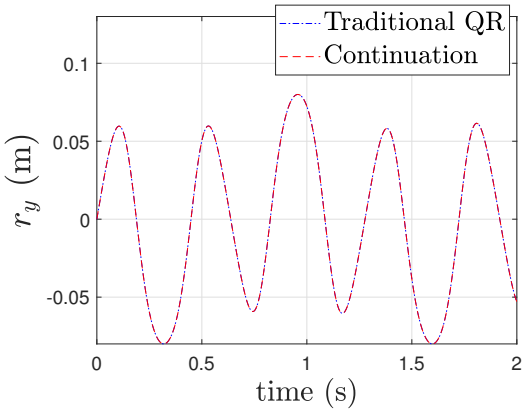

(b) The position of pendulum in y direction

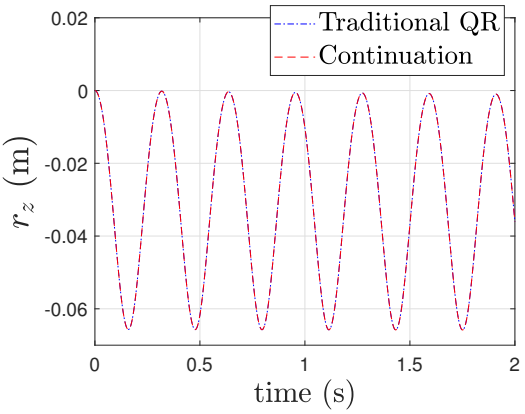

(c) The position of pendulum in z direction

Figure 5.6: Time history of the physical coordinates of the spatial pendulum

5.1.2. Comparison with MBDyn Simulation

The spatial pendulum is also simulated using high-fidelity multibody simulation, namely MBDyn[1] to check if the results are comparable to the previous simulation. This software is open source and was created with the general purpose of resolving multibody problems. The simulation uses a second-order accurate implicit linear multistep integration method with algorithmic dissipation (asymptotic spectral radius $\rho_\infty = 0.6$) [21, 22]. The result of the pendulum's position with different time steps can be seen in Fig. 5.7.

[1] https://www.mbdyn.org/

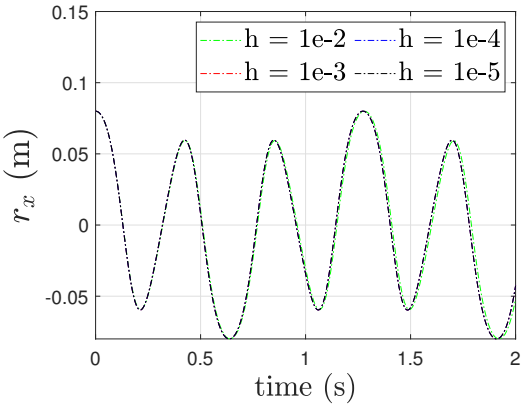

(a) The position of the pendulum in the x direction

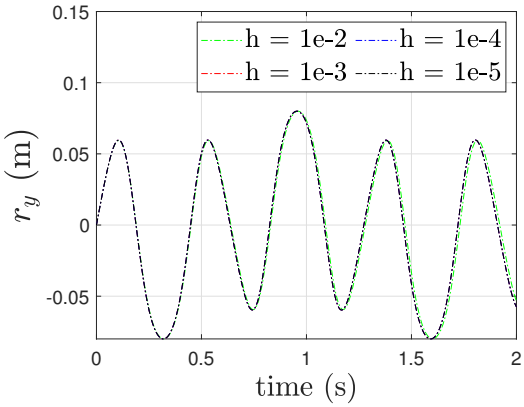

(b) The position of the pendulum in the y direction

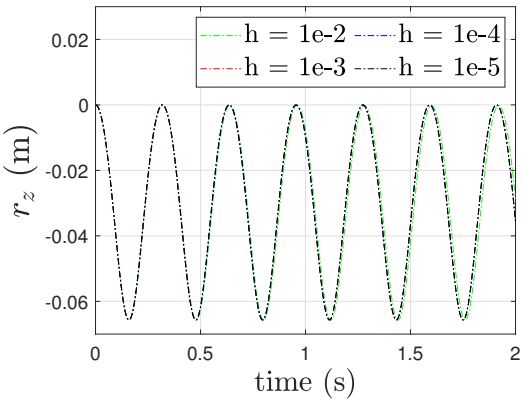

(c) The position of the pendulum in the z direction

Figure 5.7: The time history of position of the spatial pendulum obtained from DAE integration using MBDyn

Furthermore, Fig. 5.8 shows the pendulum's position in the x-direction with the specific range of time (0.999 seconds to 1.001 seconds) to see the convergence of the simulation when the time step reduces.

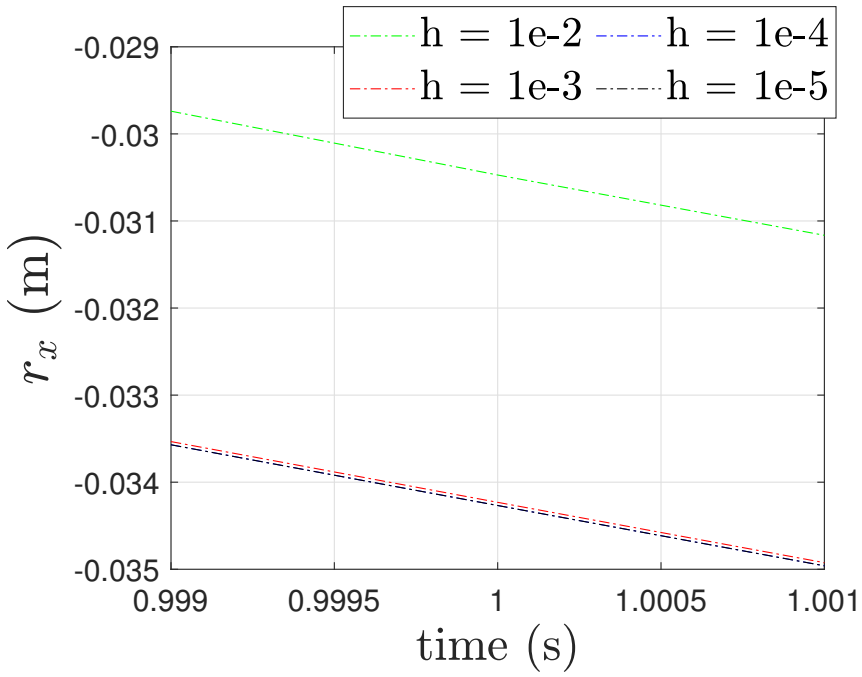

Figure 5.8: The position of the pendulum in the x direction using MBDyn for a certain time

It can be observed that with the time step h = 10^{-4} (blue line) and h = 10^{-5} (black line), the position of the pendulum over time is identical. It can be concluded that with the time step h = 10^{-4}, the simulation has reached convergence.

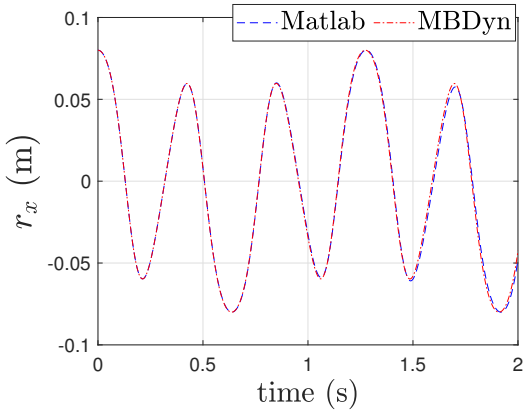

(a) The position of the pendulum in the x direction

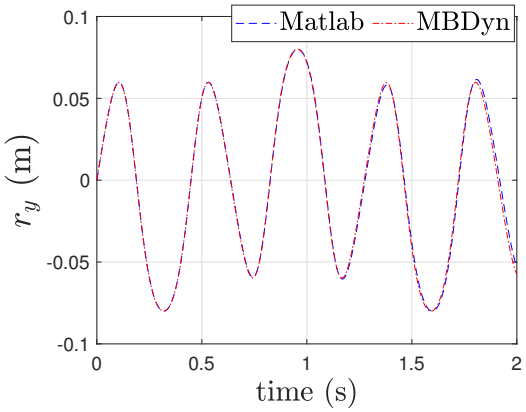

(b) The position of the pendulum in the y direction

Figure 5.9: The comparison of the time history of position of the spatial pendulum using Matlab and MBDyn

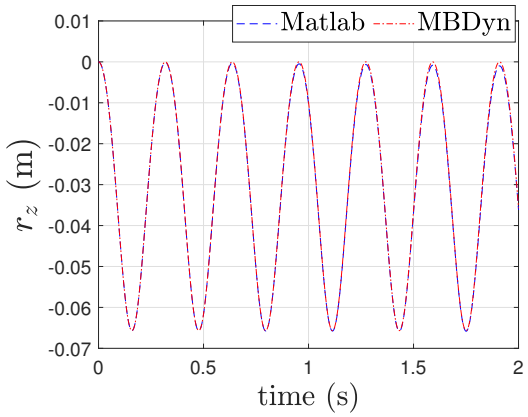

(c) The position of the pendulum in the z direction

Figure 5.9: The comparison of the time history of position of the spatial pendulum using Matlab and MBDyn

The simulation using the projection continuation method based on the QR factorization of the transpose of the Jacobian matrix using ode45 integration produces a comparable result of the trajectory of the pendulum when its compared to the simulation using high fidelity simulation MBDyn using the same time step h = 10^{-4}, as can be seen from Fig. 5.9.

5.2. 4-Bar Mechanism

This part will cover the analysis and results obtained from the simulations of a 4-bar mechanism and its modifications. This mechanism was originally proposed by IFToMM's Technical Committee for Multibody Dynamics[2]. The first mechanism presented in this thesis is a single 4-bar mechanism. Moreover, several modifications of the 4-bar mechanism will also be shown. In total, six systems will be presented. The purpose is to complete the problem by evaluating the different mechanisms. A brief summary of the description of each system can be seen in Tab. 5.1

The simulation is carried out using Matlab, especially function qr, to compute suitable matrix **T**, and function ode45 (with Relative tolerance and Absolute tolerance 10^{-6} respectively) to do the integration.

[2]https://www.iftomm-multibody.org/benchmark/problem/Double_four_bar_mechanism/

mechanism	m	n	d	description
4-bar	8	9	0	$m < n$, non-redundant, 1 dof
2 4-bar	14	15	0	$m < n$, non-redundant, 1 dof
modification of 2 4-bar	12	12	1	$m = n$, redundant, 1 dof
modification of 2×2 4-bar	24	24	2	$m = n$, redundant, > 1 dof
modification of 3 4-bar	16	15	1	$m > n$, redundant, 1 dof
modification of 2×3 4-bar	32	30	2	$m > n$, redundant, > 1 dof

Table 5.1: Brief summary of the simulated systems

First, consider the 4-bar mechanism connected using a revolute joint as shown in Figure 5.10. All bars have a length of 1 m. The mass of all bars is the same, namely 1 kg. The inertial moment of all bars is $\frac{1}{12}$ kg/m^2. The gravity, $g = 9.81$ m/s^2, applies in this mechanism downward. The system has nine ordinary differential equations ($n = 9$) and eight constraints ($m = 8$).

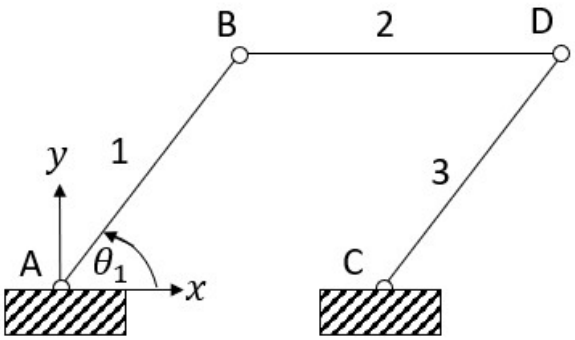

Figure 5.10: 4-Bar mechanism

Assume all the bars are homogeneous, so the center of mass of each bar is in the middle. The initial position bars number 1 and 3 are $\theta_1 = \theta_3 = \frac{1}{2}\pi$ rad, and the initial angular velocity of bars number 1, 2, and 3 are 4, 0, and 4 rad/s, respectively.

The simulation is done for 2 seconds with time step, h $= 10^{-4}$ seconds. The time history of an angle of bars no. 1 and 3 are displayed in Figure 5.11.

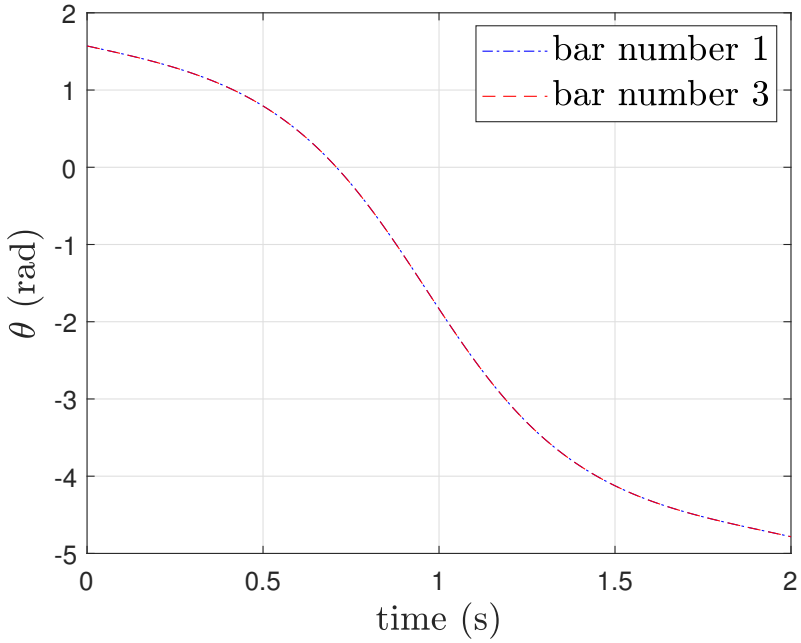

Figure 5.11: The time history of the angle of bars no. 1 and 3 of the 4-bar mechanism

Moreover, the angular speed of bars 1 and 3 are shown in Figure 5.12.

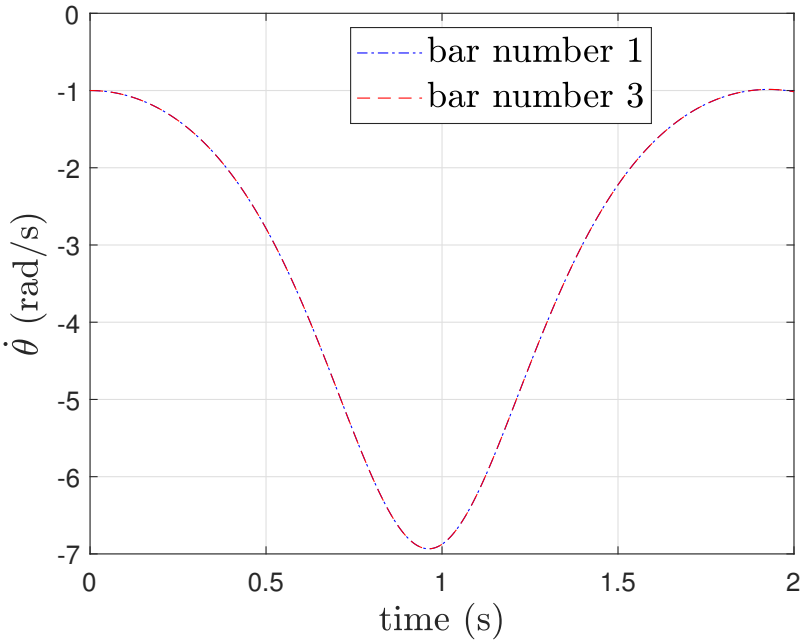

Figure 5.12: The time history of the angular speed of bars no. 1 and 3 of the 4-bar mechanism

Based on Fig. 5.11 and Fig. 5.12, it can be observed that the movement of the two bars is

identical, in other words, the position and velocity of those bars are the same every time.

Furthermore, Fig. 5.13 shows the movement of r_{2y} and θ_2. It is mentioned that when the vertical position of bar no. 2 is zero meaning all bars are in a horizontal position, a singularity condition appears.

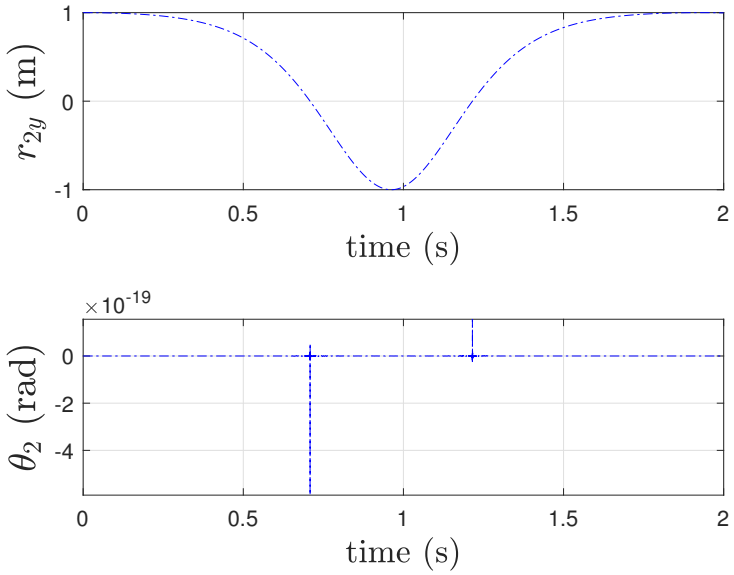

Figure 5.13: The time history of vertical position and angle on bar no. 2 of the 4-bar mechanism

5.2.1. Continuation Algorithm for the 4-Bar Mechanism

This part will use the continuation algorithm to make the generalized coordinates have continuous values each time. The comparison of projected generalized velocities, $\dot{\mathbf{q}}$, with and without the continuation algorithm can be seen in Fig. 5.14.

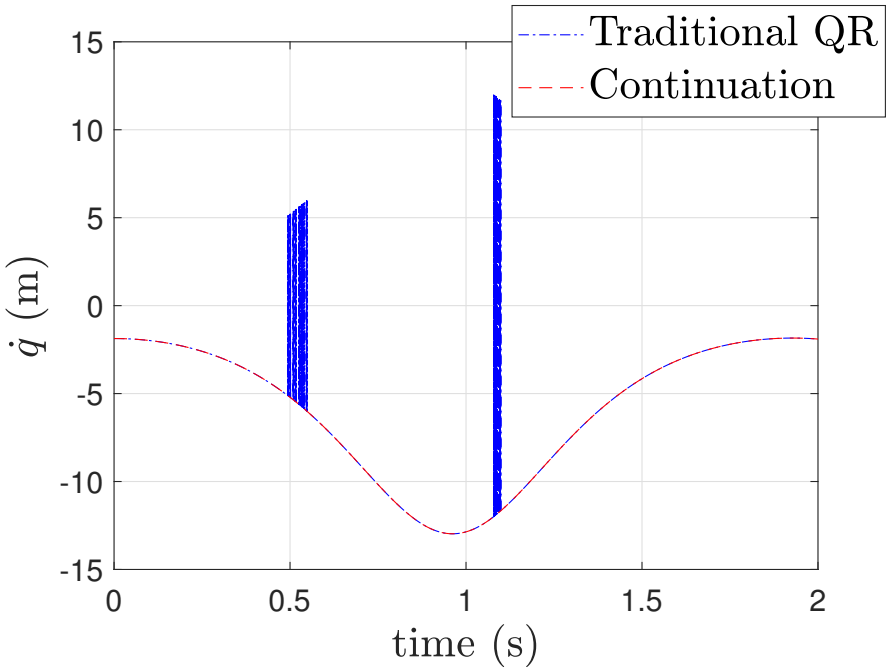

Figure 5.14: Time history of projected velocities, $\dot{\mathbf{q}}$, of the 4-bar mechanism

As mentioned before, using the continuation approach, the time history of the projected generalized velocities is continuous. Whereas if using traditional QR, the result of $\dot{\mathbf{q}}$ is discontinuous. In other words, its value sometimes experiences a sudden and uncontrollable sign change whenever it occurs.

Both algorithms start from a negative sign (see Fig. 5.14) since the two approaches were initialized in the same manner through Matlab's QR factorization and the same constraint Jacobian matrix. With the continuation, the sign is consistent. Whereas with the traditional one, it occasionally turns to positive and then negative again because of the blind execution of the QR factorization algorithm.

Furthermore, the singularity condition could be seen by evaluating the diagonal elements of matrix $\mathbf{R}_1$. As displayed in Fig. 5.15, the last diagonal elements of matrix $\mathbf{R}_1$ drop to zero, or close to zero, when the singularity appears.

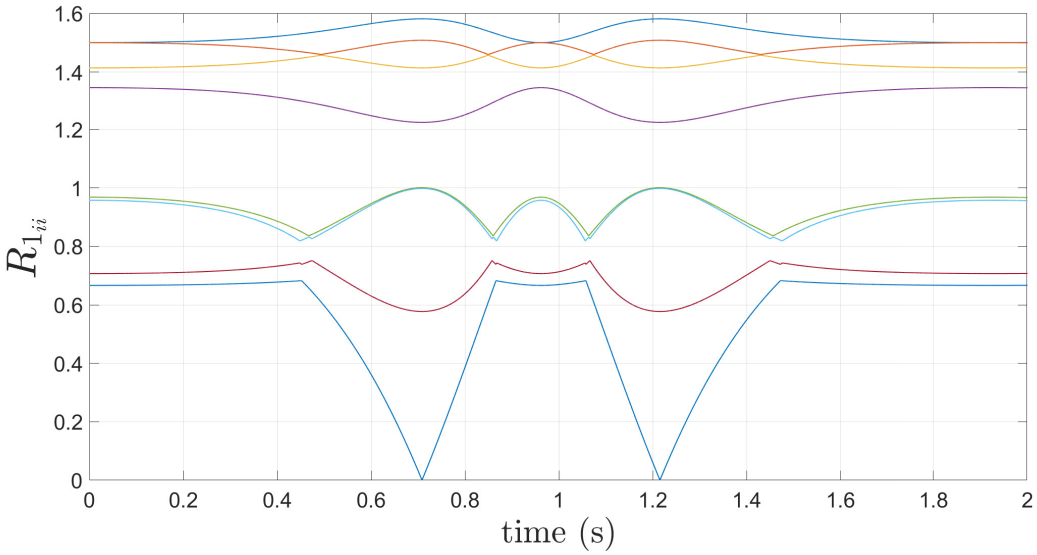

Figure 5.15: Time history of the diagonal coefficient of matrix $\mathbf{R}_1$ of the 4-bar mechanism

Fig. 5.16 shows only the time history of the diagonal part of matrix $\mathbf{R}_1$ whose value goes to zero.

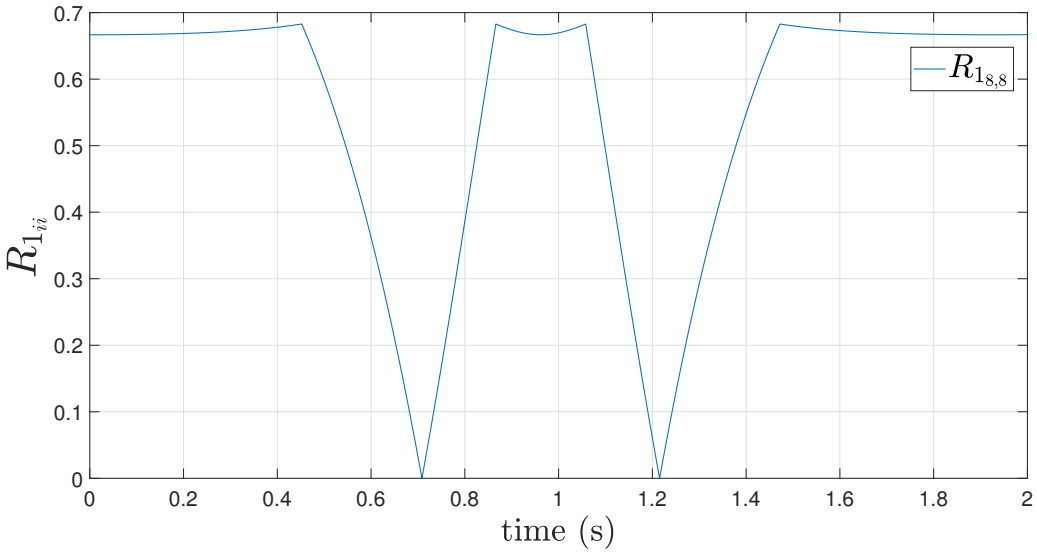

Figure 5.16: Time history of the last diagonal coefficient of matrix $\mathbf{R}_1$ of the 4-bar mechanism

When the singularity condition arises, the mechanism undergoes other possible movements regardless of the initial one. The second motion can be easily captured by evaluating matrix $\mathbf{T}$. Fig. 5.17 shows the value of the matrix in the singularity condition.

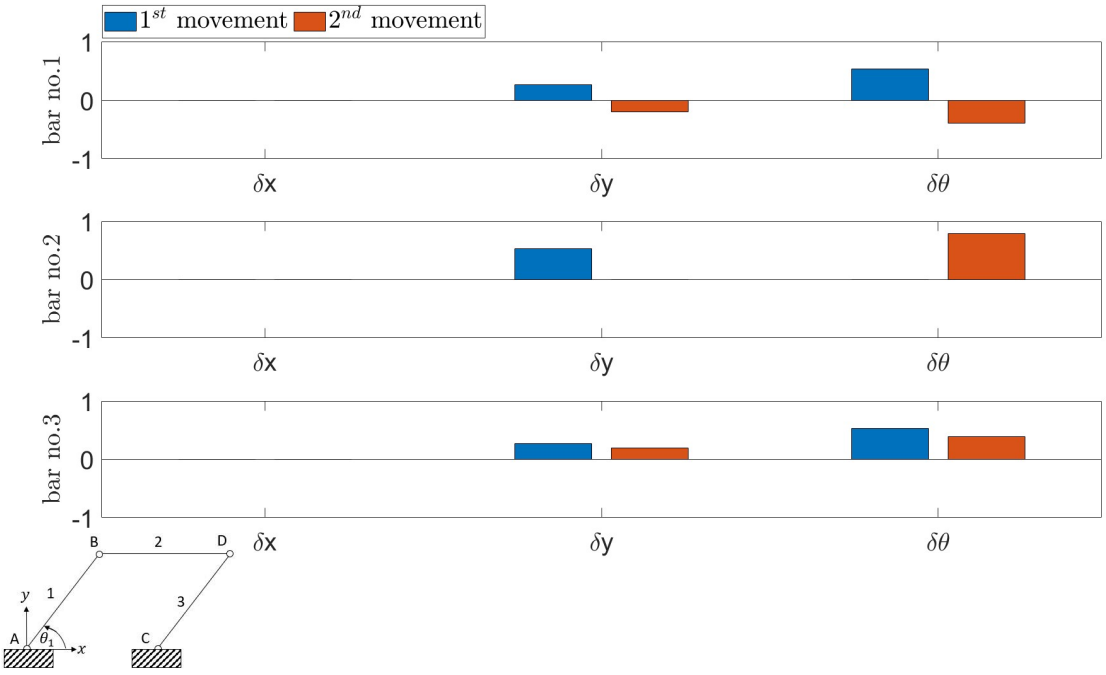

Figure 5.17: 4-bar mechanism: the values of the suitable matrix **T** at singularity condition

An intuitive image of how the bar moves can be seen in Fig. 5.18.

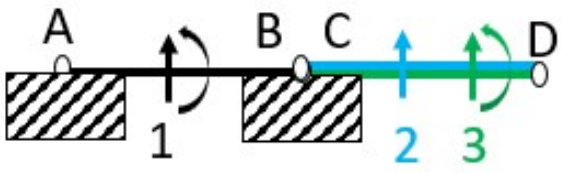

(a) 1st movement

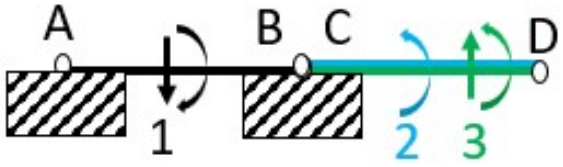

(b) 2nd movement

Figure 5.18: Possible movement of the 4-bar mechanism at singularity condition

5.2.2. Singularity Evaluation for the 4-Bar Mechanism

Consider the previous 4-bar mechanism system. The system is given a certain speed such that it will stop when all bars are in a horizontal position. Bars number 1 and 3 are given an initial angular velocity of -4.8522 rad/s, and bar number 2 is 0 rad/s. The initial

position for bar no. 1 is $\theta_1 = \frac{3}{2}\pi$ rad. The result shows in Figure 5.19

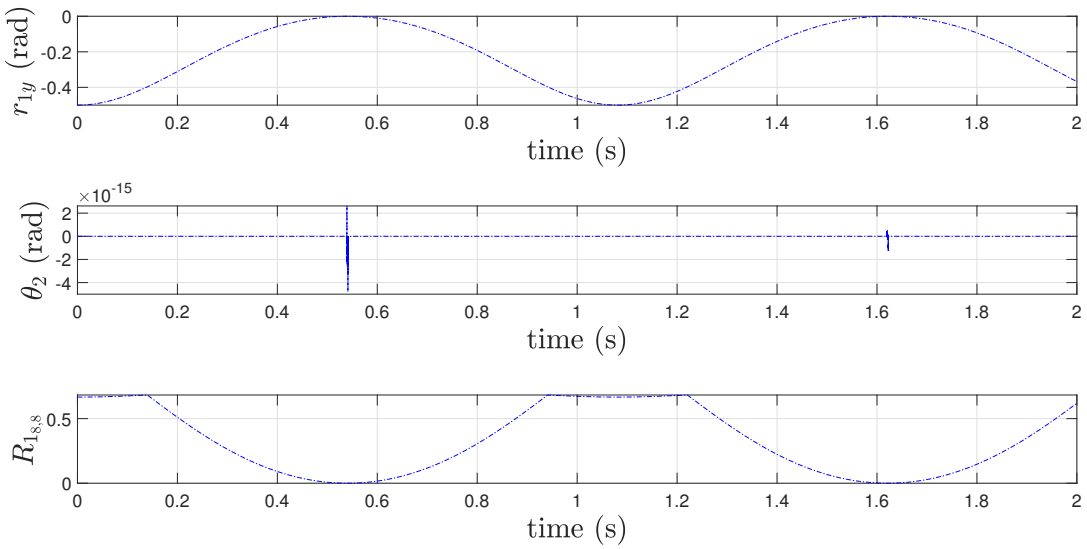

Figure 5.19: 4-bar mechanism stopping at horizontal

It can be noticed that when all bars are in the horizontal position, the value of the last diagonal of matrix $\mathbf{R}_1$ drops to zero. It can also be observed that the value of that matrix goes to zero at a gentle speed. This can be explained by understanding that the system will physically stop at that moment. The angle of bar number 2 also undergoes an abrupt change at that moment. In other words, it can be said that the system is in a singularity condition. At this moment, the system has the possibility to make other moves that are different from the previous motion.

Introducing the second movement of the system could be done by adding a specific torque in bar number 2. For this moment, the added torque is -20 Nm to trigger the other movement of the 4-bar mechanism. The result for the time history of θ_1, θ_2, and θ_3 is displayed in Fig. 5.20.

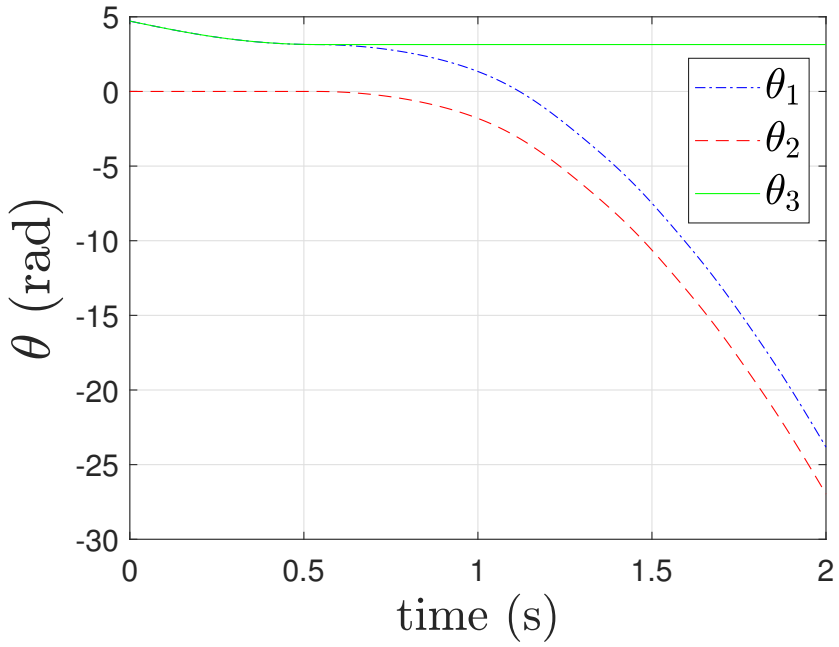

Figure 5.20: Time history of θ_1, θ_2, and θ_3 of the 4-bar mechanism

From Fig. 5.20, it is observed that the movement of bars number 1, 2, and 3 are not the same anymore. Instead, they move in different directions.

Furthermore, the time history of the last diagonal value of $\mathbf{R}_1$ is shown in Figure 5.21.

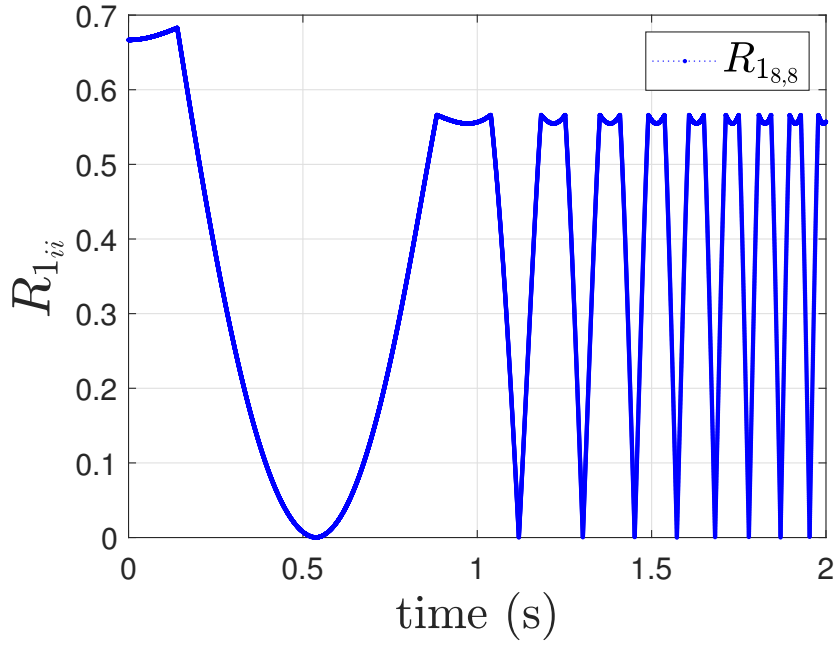

Figure 5.21: Time history of the diagonal coefficients of matrix $\mathbf{R}_1$ of the 4-bar mechanism

5.3. 2 4-Bar Mechanisms

This mechanism is a modification of the 4-bar system where this system is added with two more bars (4 and 5). Those bars are identical to the bars in the previous mechanism. The connection between bars number 2 and 4 is a revolute joint, so both are independent, as displayed in Fig. 5.22. The system has 15 ordinary differential equations (n) and 14 constraints (m).

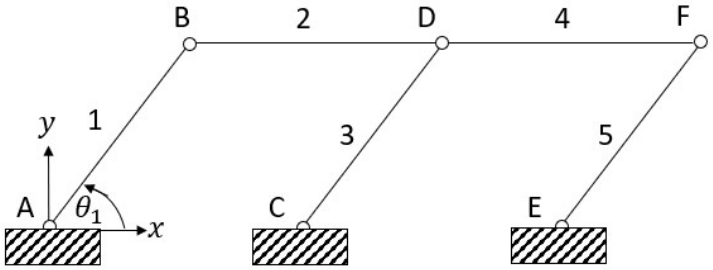

Figure 5.22: 2 4-Bar mechanism

Applying the previous initial condition to bars number 1, 3, and 5, the results of 2 seconds simulation with time steps (h = 10^{-4}) are shown in the images below.

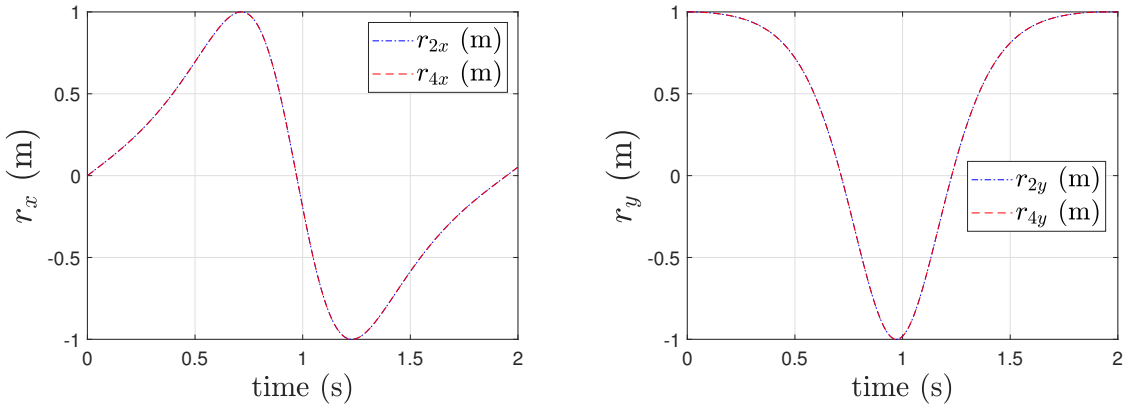

(a) The horizontal position of bar no. 2 and 4 (b) The vertical position of bar no. 2 and 4

Figure 5.23: Time history of the position of bars no. 2 and 4 in the 2 4-bar mechanism

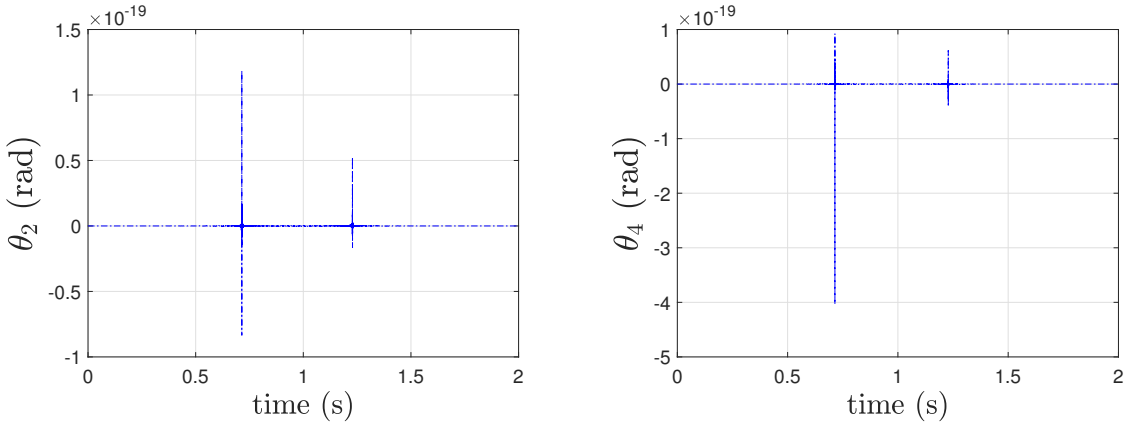

(a) The angle of bar no. 2 over time (b) The angle of bar no. 4 over time

Figure 5.24: Time history of the rotation angle of bars no. 2 and 4 in the 2 4-bar mechanism

It can be seen that the motion of two bars (2 and 4) are identical. Then, when all bars are in the horizontal position (can be observed from Fig. 5.23b), the system experiences singularity configuration, θ_2 and θ_4 experiences a sudden jump in value.

Compared to the previous mechanism, although the motion is not exactly the same, the motion of bar number 2 in this mechanism is identical to the previous mechanism. It is because the double 4-bar mechanism has more inertia compared to the 4-bar mechanism. Fig. 5.25 shows the comparison of the position of the 4-bar mechanism and 2 4-bar mechanisms in the x and y-direction.

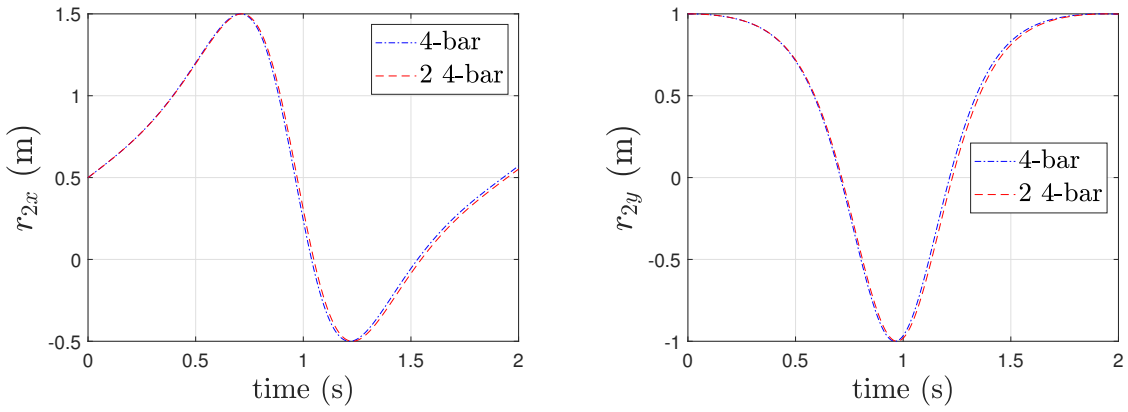

(a) Time history of the horizontal position of bar no. 2 (b) Time history of the vertical position of bar no. 2

Figure 5.25: The comparison of the position of bar no.2 between 4-bar and 2 4-bar mechanisms

5.3.1. Continuation Algorithm for the 2 4-Bar Mechanisms

The time history of $\dot{\mathbf{q}}$ using the continuation algorithm can be seen in Fig. 5.26.

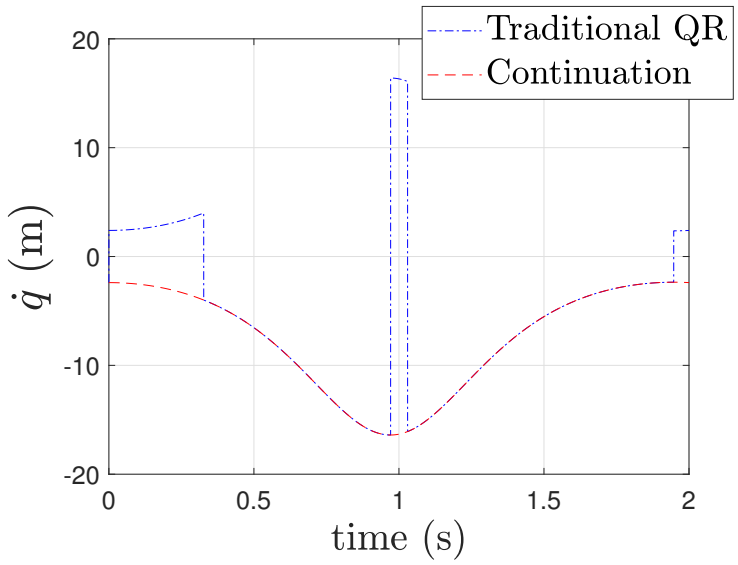

Figure 5.26: Time history of the projected velocities, $\dot{\mathbf{q}}$, of the 2 4-bar mechanisms

The time history of the diagonal coefficients of matrix $\mathbf{R}_1$ can be seen in Fig. 5.27.

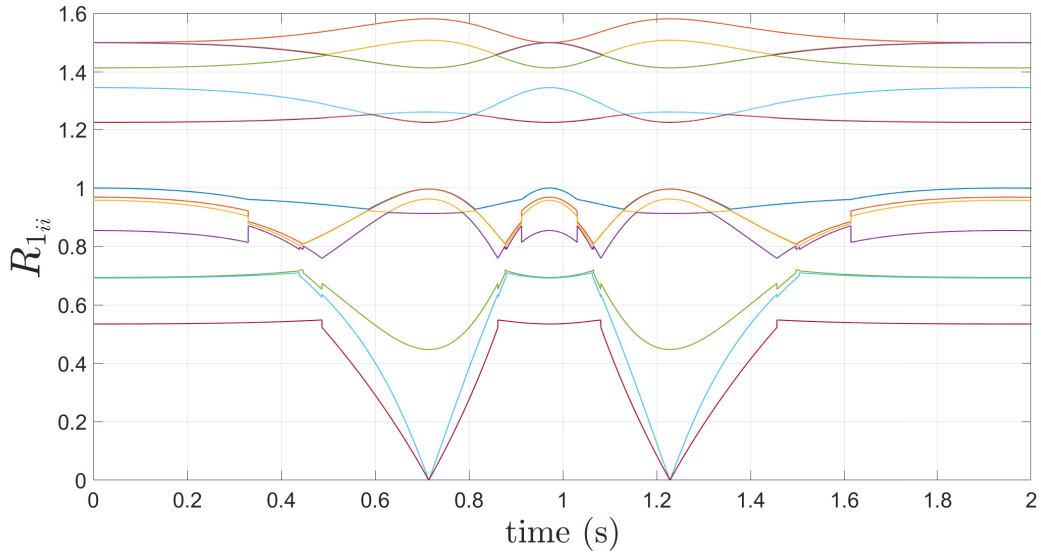

Figure 5.27: The time history of the diagonal coefficients of matrix $\mathbf{R}_1$ of the 2 4-bar mechanisms

It can be observed that two diagonal values go to zero when the system experiences the singularity condition. This means that the degree of freedom of the mechanism is changed.

It increases from 1 dof to 3 dof. The system has the possibility to make different motions from the previous one. The other movement can be easily seen by checking the values of matrix **T** at the singularity condition.

Fig. 5.28 shows the value of matrix **T** when a singularity occurs. It notices that the system experiences two additional motions in addition to the expected motion.

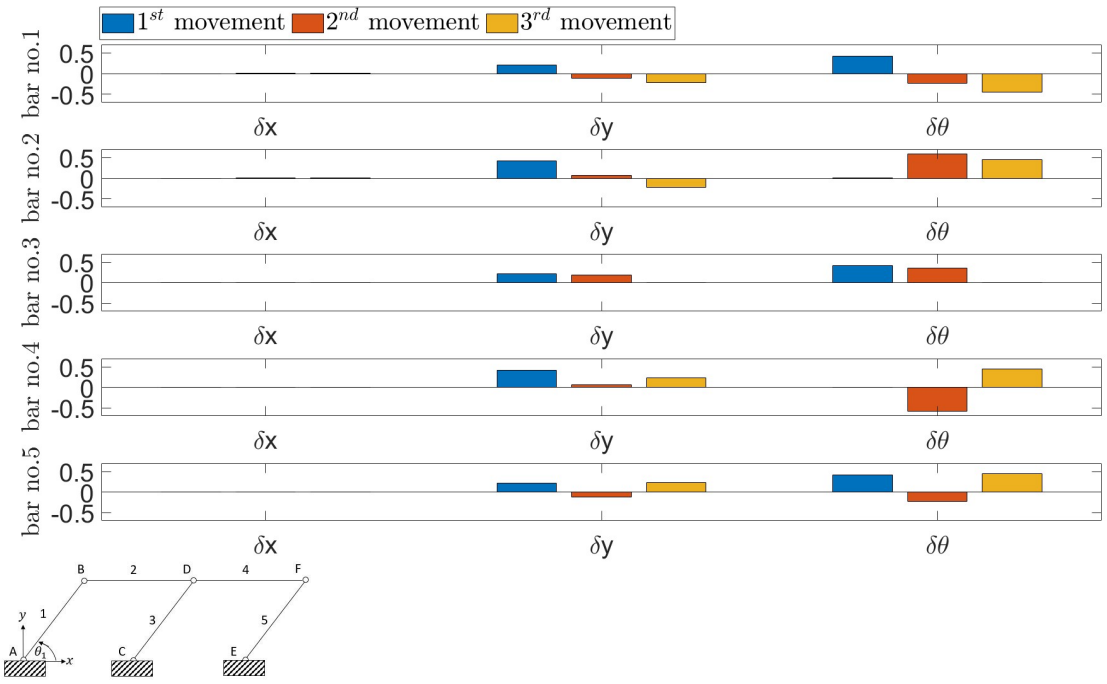

Figure 5.28: The values of the suitable matrix **T** at singularity condition of the 2 4-bar mechanisms

A more intuitive visualization to capture the possible motion in singularity condition can be seen in Fig. 5.29.

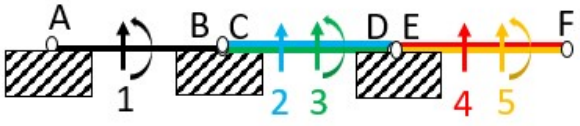

(a) 1st movement

(b) 2nd movement

(c) 3rd movement

Figure 5.29: Possible movement of the 2 4-bar mechanisms

5.4. Modified Form of the 2 4-Bar Mechanisms

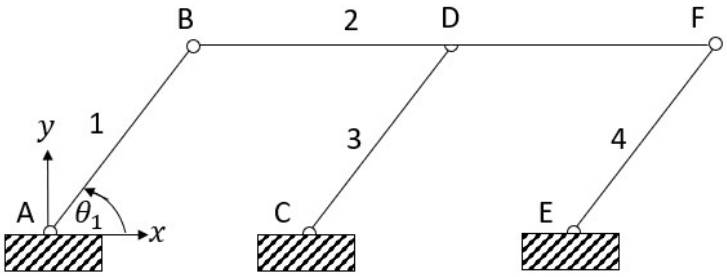

Figure 5.30: 2 4-Bar mechanisms modified form

Using the previous double 4-bar mechanisms, but with a modification in bar BD and DF. The two are now connected rigidly in D to form a single part (it is called bar number 2). The mass and length of that bar are 2 kg and 2 m. Thus, the moment of inertia is $\frac{2}{3}$ kg/m^2. Furthermore, this system has 12 ordinary differential equations, and it is the same as its number of constraints ($m = n$). However, because of the rank deficiency of the jacobian matrix of this system, $d = 1$, this mechanism has one degree of freedom.

The system is simulated by giving the initial angular velocity of -1 rad/s to bars number 1, 3, and 4. The time history of the position of bar no. 1 for the 2 seconds simulation can be seen in Fig. 5.31

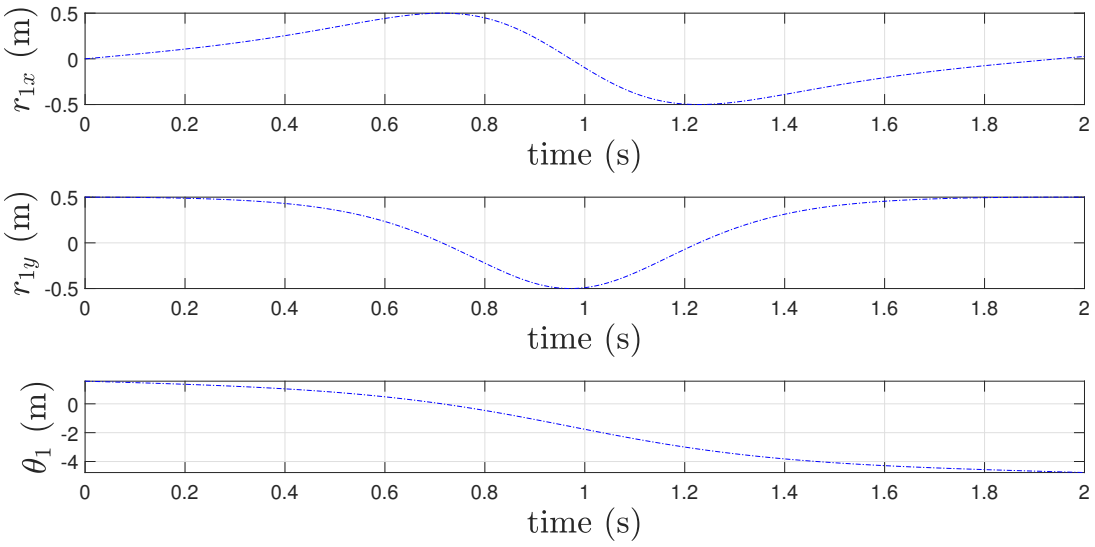

Figure 5.31: Time history of the position of bar no. 1 of the modified form of the 2 4-bar mechanisms

Furthermore, the figures below show the comparison of 2 4-bar mechanisms without and with modification.

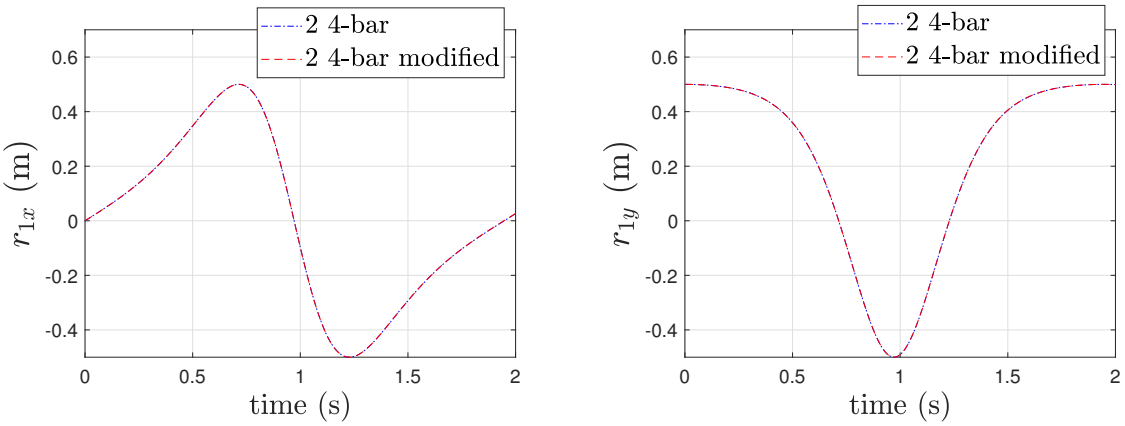

(a) Time history of the horizontal position of bar no. 2

(b) Time history of the vertical position of bar no. 2

Figure 5.32: The comparison of the position of 2 4-bar without and with modification

It can be observed that the position of bar number 1 of those systems is identical over the simulation. It can be concluded that the whole motion of those systems is comparable.

5.4.1. Continuation Algorithm for Modified Form of the 2 4-Bar Mechanisms

This part presents the results of the modified form of 2 4-bar mechanisms using the continuation algorithm. This algorithm obtains the same result as traditional QR in terms of physical coordinates, as shown in Fig. 5.33. This figure shows the results of the position of bar number 1 using traditional QR and continuation.

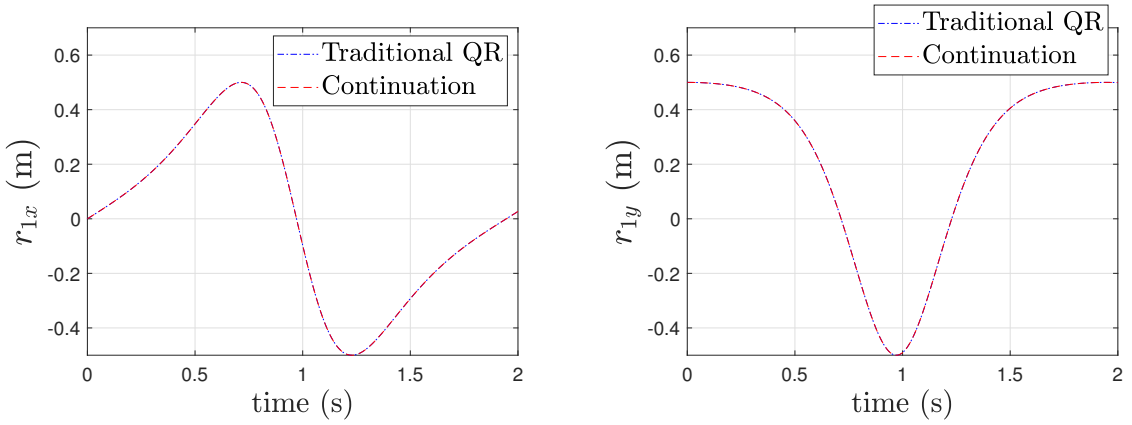

(a) Time history of the horizontal position

(b) Time history of the vertical position

Figure 5.33: Time history of the position of bar no. 1 of the modified form of the 2 4-bar mechanisms

However, the continuation algorithm yields the projected velocity becoming continuous over time. Whereas using traditional QR, the values of $\dot{\mathbf{q}}$ are discontinuous, as shown in Fig. 5.34. This figure demonstrates the result of projected generalized velocity using traditional QR and continuation.

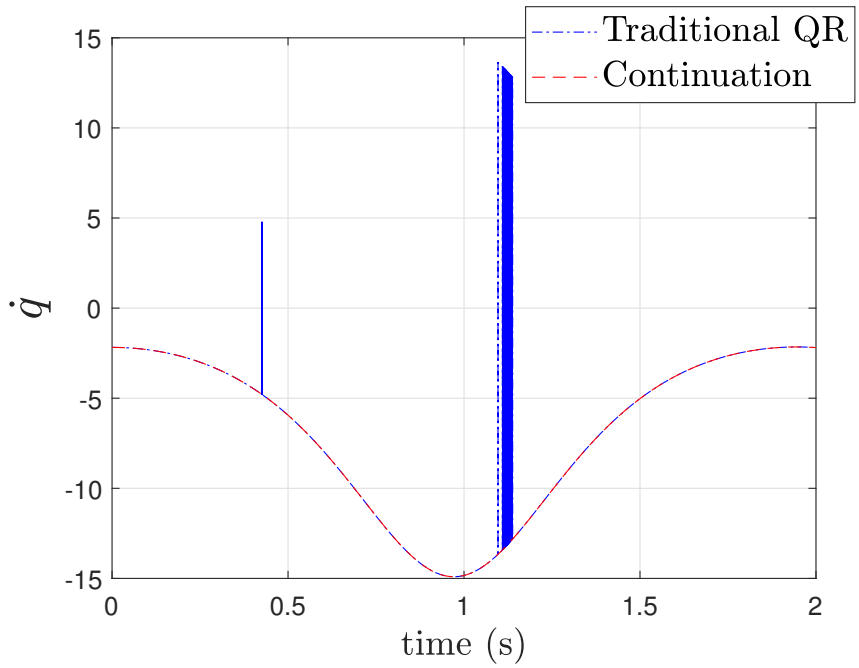

Figure 5.34: The time history of the projected velocity of the modified form of the 2 4-bar mechanisms

Furthermore, the time history of the suitable matrix **T** related to the bar number 1 using traditional QR and continuation can be observed respectively in Fig. 5.35 and Fig. 5.36.

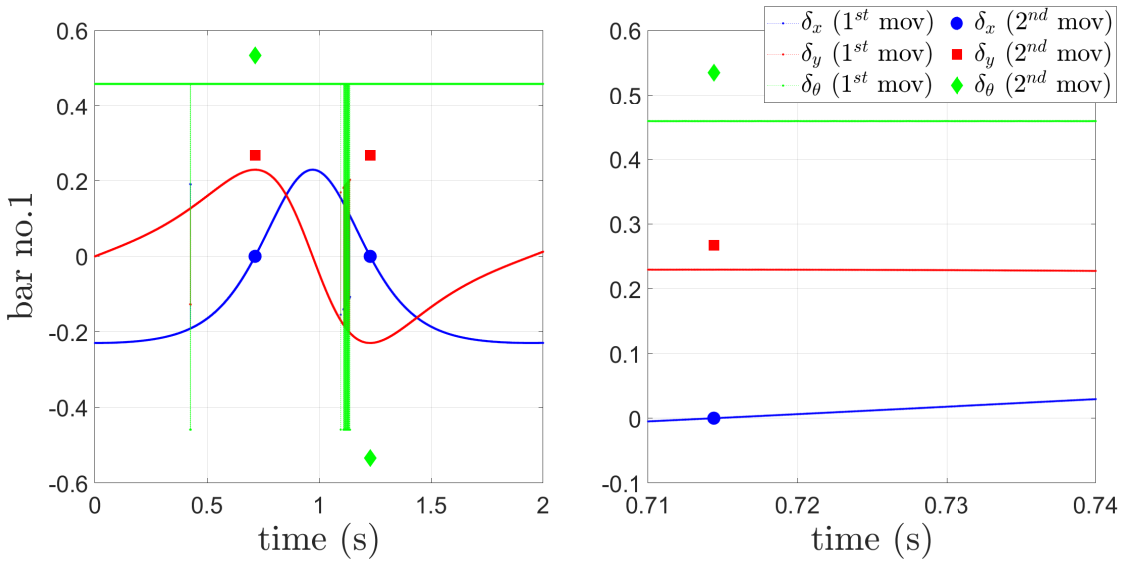

Figure 5.35: Time history of suitable matrix **T**(1:3,:) with traditional QR of the modified form of the 2 4-bar mechanisms

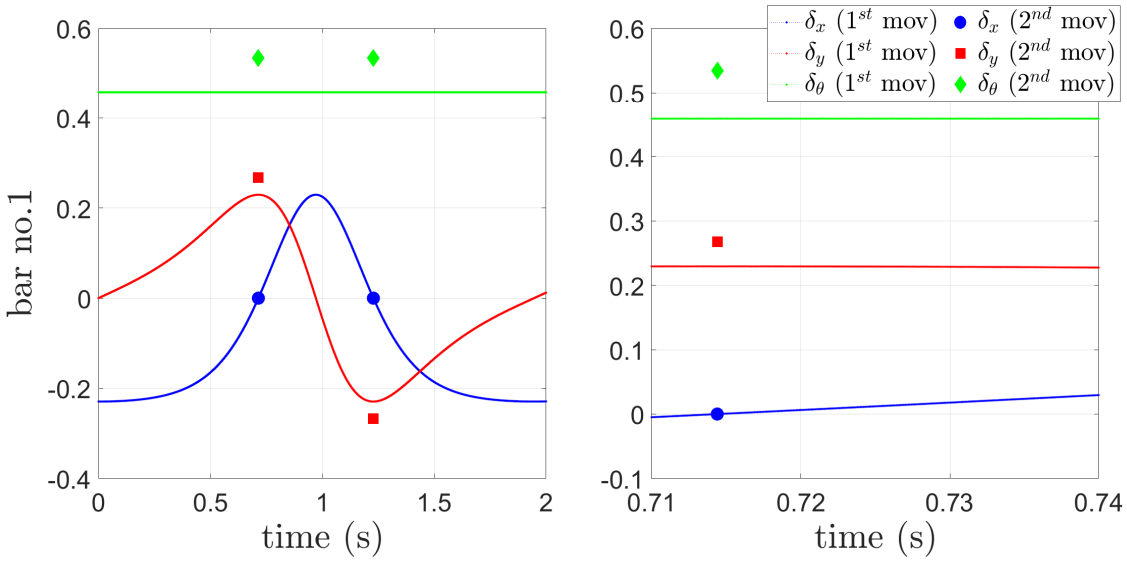

Figure 5.36: Time history of suitable matrix $\mathbf{T}(1{:}3,:)$ with continuation of the modified form of the 2 4-bar mechanisms

From the two figures above, it can be seen that the values of matrix $\mathbf{T}$ in the continuation algorithm are continuous. It is also observed that when the singularity occurs, matrix $\mathbf{T}$ will produce other values. Because when the singularity condition appears, the rank of the Jacobian matrix is reduced.

Furthermore, Fig. 5.37 shows all the diagonal values of matrix $\mathbf{R}_1$.

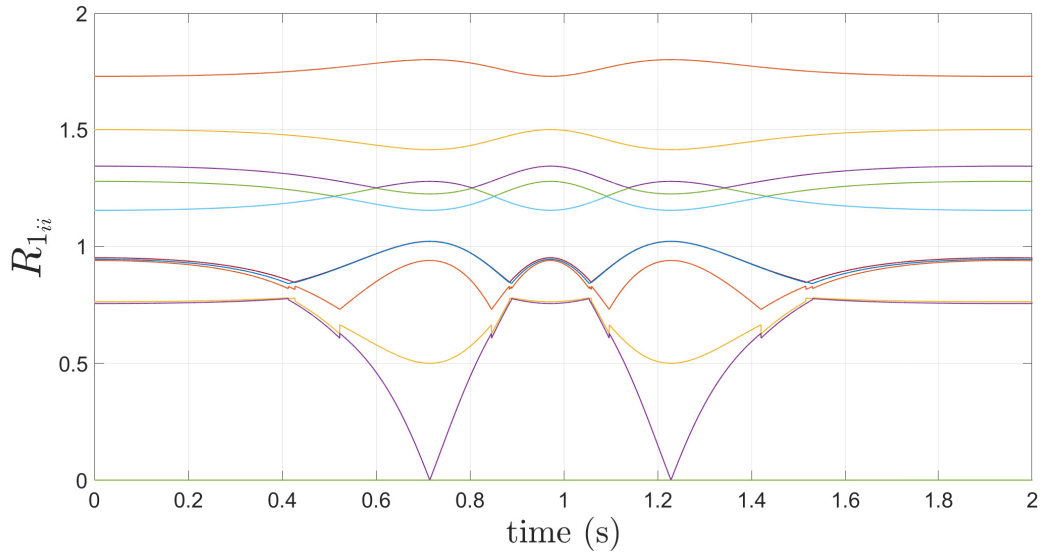

Figure 5.37: The time history of the diagonal coefficient of matrix $\mathbf{R}_1$ of the modified form of the 2 4-bar mechanisms

When the system experiences a singularity condition, some component of the diagonal coefficients of $\mathbf{R}_1$ will move towards zero. Evaluating the values of matrix $\mathbf{T}$ in this condition will reveal another possible motion of the system, as mentioned before. Fig. 5.38 shows the value of matrix $\mathbf{T}$ when a singularity occurs.

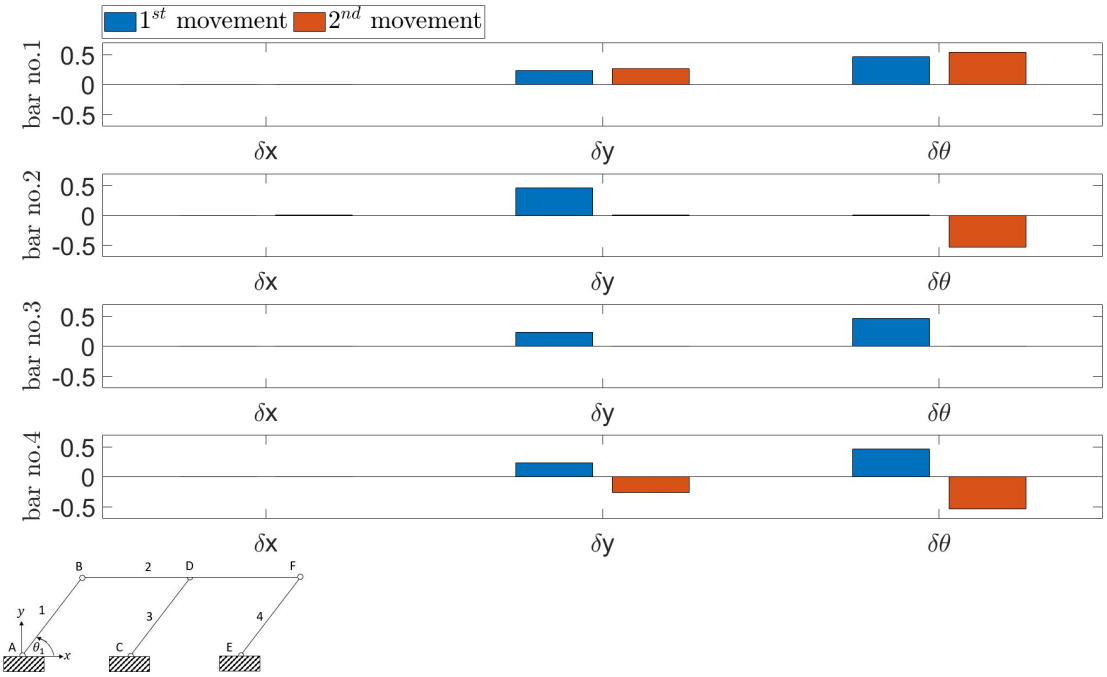

Figure 5.38: Possible movement of the modified form of the 2 4-bar mechanisms

A more intuitive figure which shows the possible motion of all bars is displayed in Fig. 5.39.

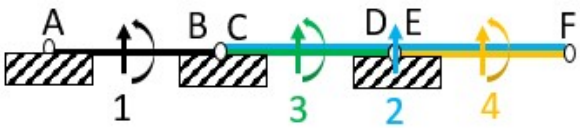

(a) 1st movement

(b) 2nd movement

Figure 5.39: Possible movement of the modified form of the 2 4-bar mechanisms

5.5. Modified Form of the 2×2 4-Bar Mechanisms

Modifying the 2 4-bar mechanisms by adding another 2 4-bar mechanisms with the same properties as the previous one. This simulation is carried out to evaluate a system that has a redundant constraint and more than 1 degree of freedom and analyse how the singularity condition occurs in that system.

The system is given initial condition for θ_1 and θ_5 are equal with $\frac{\pi}{2}$. The initial angular velocities for bars number 2 and 6 is zero. The remaining bars have the intial angular velocities of -1 rad/s.

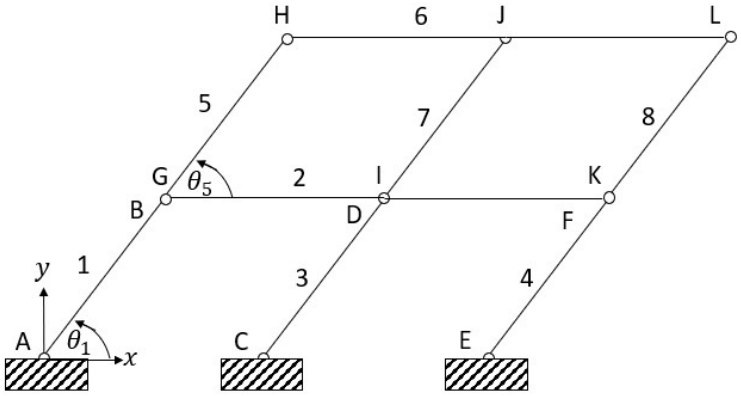

Figure 5.40: 2×2 4-bar mechanisms

The system is simulated for 2 seconds. The result for the position of bars number 1 and 5 is shown in Fig. 5.41.

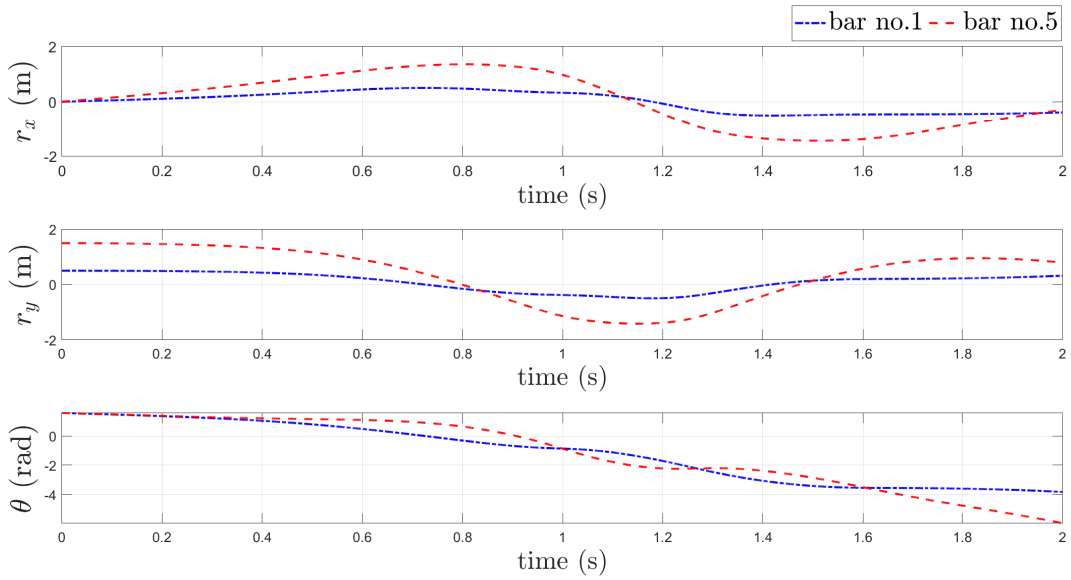

Figure 5.41: Time history of bar no. 1 and 5 of the modified form of the 2×2 4-bar mechanisms

It can be observed that the first 2 4-bar mechanisms (bars number 1, 2, 3, and 4) reach the horizontal position (for all bars) is different from the second 2 4-bar mechanisms (bars number 5, 6, 7, and 8). This also explains the part of matrix $\mathbf{R}_1$ that goes to zero between 0.6 seconds and 1 second twice. It shows in Fig. 5.42, in which the time history of the diagonal coefficients of matrix $\mathbf{R}_1$ is displayed.

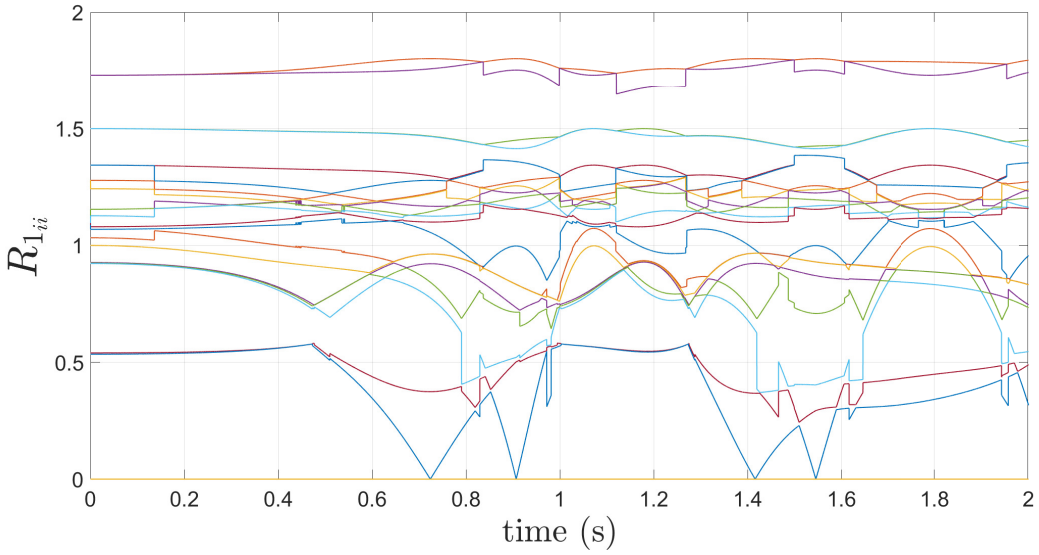

Figure 5.42: Time history of diagonal elements of matrix R_1 of modified form of the 2×2 4-bar mechanisms

5.5.1. Continuation Algorithm for Modified Form of the 2×2 4-Bar Mechanisms

Applying the continuation algorithm generates the results in the generalized coordinates, and the projected generalized velocities are progressive as compared to the traditional QR. The time history of generalized coordinates can be seen in Fig 5.43

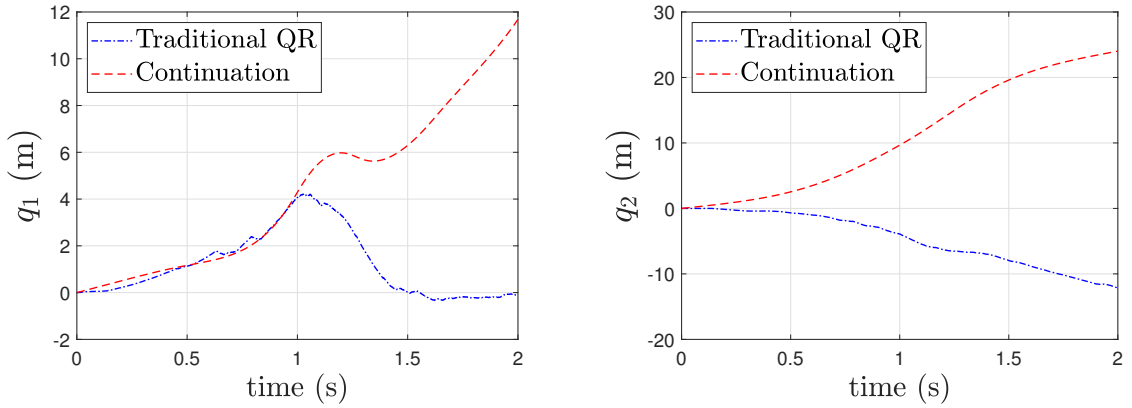

(a) Time history of q_1 (b) Time history of q_2

Figure 5.43: Time history of the generalized coordinates of the modified form of the 2×2 4-bar mechanisms

Furthermore, the projected generalized velocities can be observed in Fig. 5.44

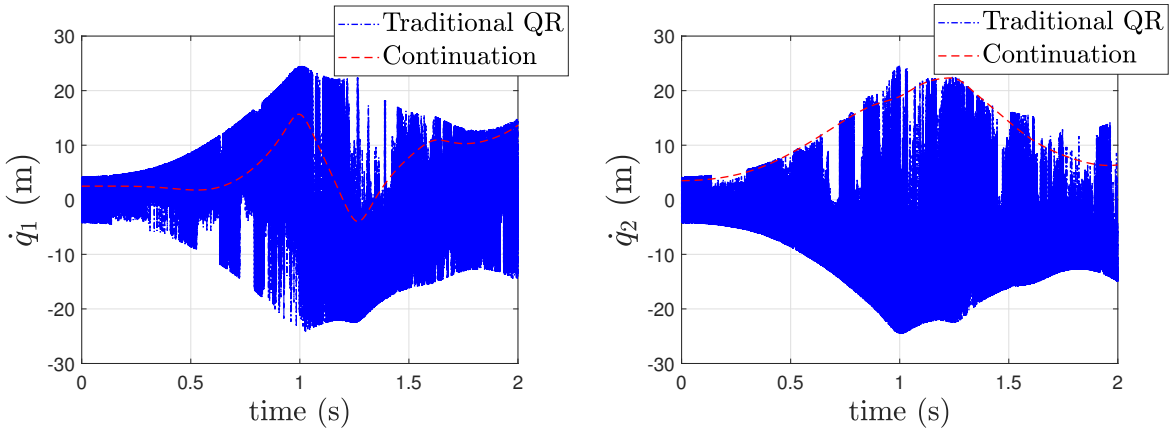

(a) Time history of $\dot{q}_1$ (b) Time history of $\dot{q}_2$

Figure 5.44: Time history of the projected velocities of the modified form of the 2×2 4-bar mechanisms

5.6. Modified Form of the 3 4-Bar Mechanisms

In this part, consider the triple 4-bar mechanisms with bar number 2 as a single bar, as shown in the figure below.

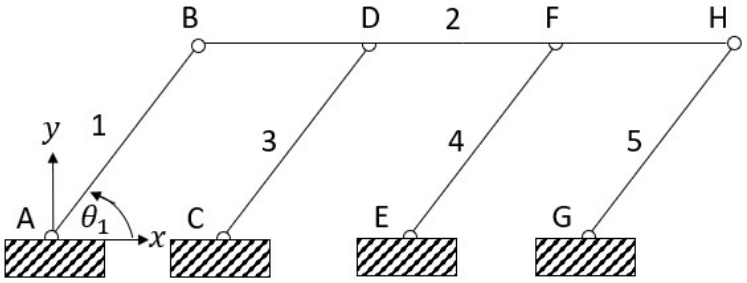

Figure 5.45: 3 4-bar mechanism

The properties of bars number 1, 3, 4, and 5 are identical, namely 1 m of the length, 1 kg of the mass, and $\frac{1}{12}$ kg/m^2 of the inertial moment. Besides that, the mass of bar number 2 is 3 kg, and the length is 3 m. The inertial moment of this bar is 2.25 kg/m^2. The initial angular velocity of this system is -1 rad/s, and it is applied to bars number 1, 3, 4, and 5. Whereas the angular speed of bar number 2 is 0 rad/s. The initial position of bars number 1, 3, 4, and 5 are $\frac{\pi}{2}$. Furthermore, the position of point D is in the $\frac{1}{3}$ of bar number 2, and point F is in the $\frac{2}{3}$ of bar number 2.

Fig. 5.46 shows the time history of bar number 2. It can be observed that when all the bars are in the horizontal position, the value of θ_2 suddenly changes. It can be understood that the system experiences the singularity condition.

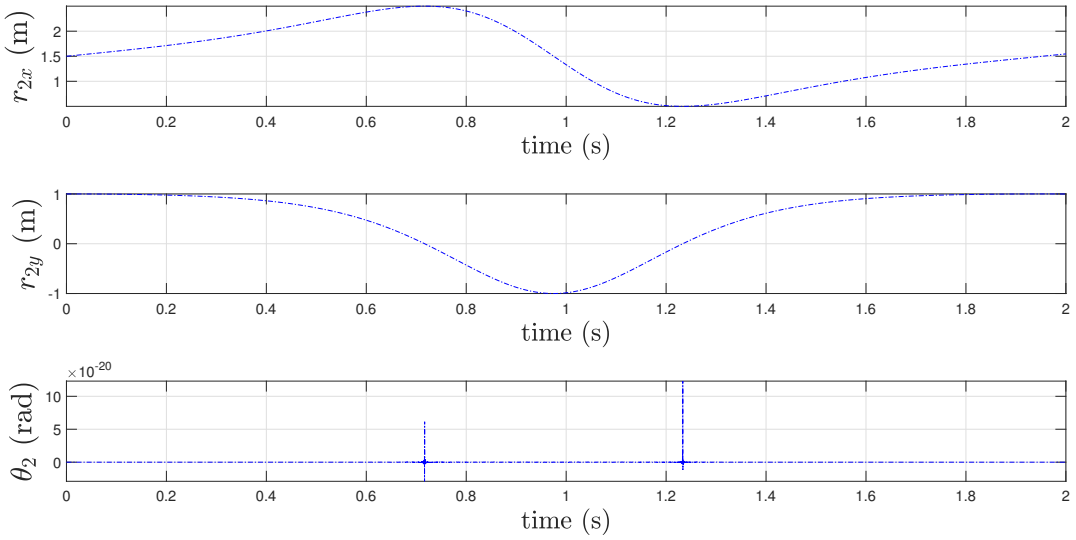

Figure 5.46: Time history of the position of bar no.2 of the modified form of the 3 4-bar mechanisms

5.6.1. Continuation Algorithm for Modified Form of the 3 4-Bar Mechanisms

This part adopts the continuation algorithm. It can be observed in Fig. 5.47 that the physical coordinates using two algorithms (traditional QR and continuation) have the same result.

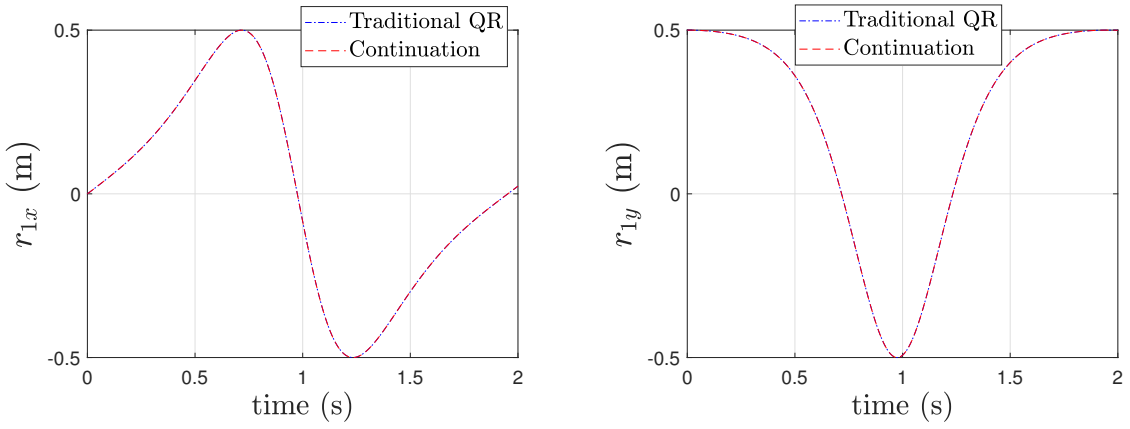

(a) The time history of the horizontal position (b) The time history of the vertical position

Figure 5.47: The time history of the position of bar no. 1 of the modified form of the 3 4-bar mechanisms

Besides that, Fig. 5.48 illustrates the comparison of the time history of the projected

generalized velocities, $\dot{q}$. It can be seen that using the continuation algorithm, the values of $\dot{q}$ over time are continuous.

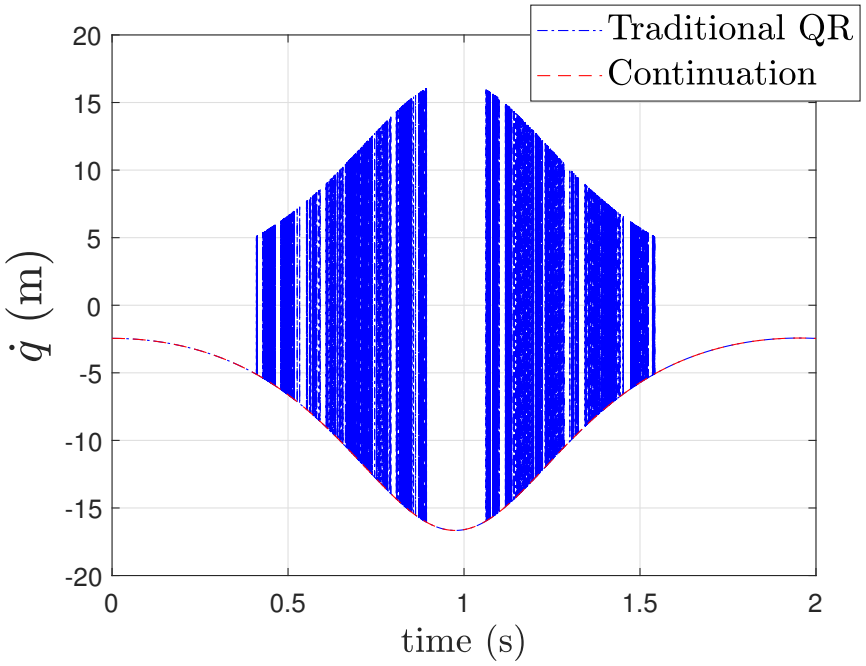

Figure 5.48: Time history of projected velocities of the modified form of the 3 4-bar mechanisms

The continuity of the result using the continuation algorithm can also be seen in matrix **T**. Fig. 5.49 and Fig. 5.50 display the first three rows of the value of matrix **T** using traditional QR and continuation, respectively.

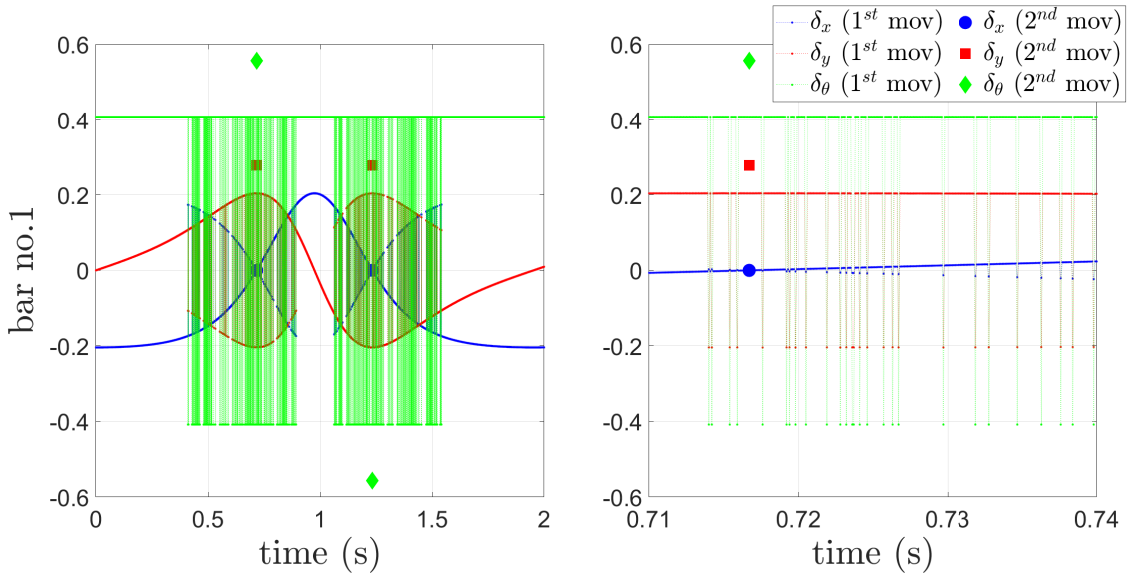

Figure 5.49: Time history of suitable matrix $\mathbf{T}(1{:}3,:)$ of the modified form of the 3 4-bar mechanisms with traditional QR

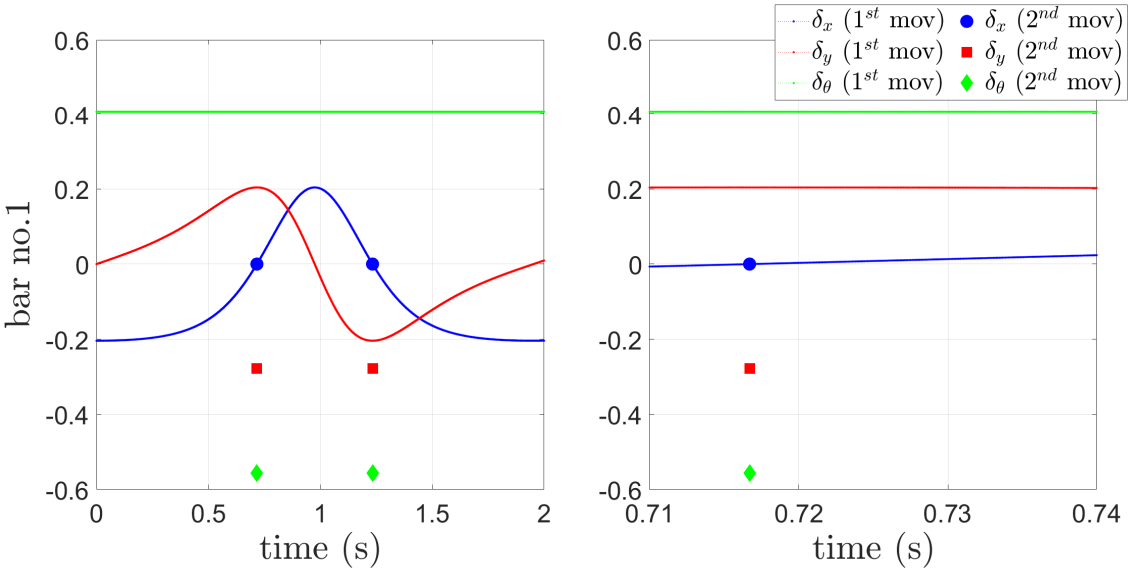

Figure 5.50: Time history of suitable matrix $\mathbf{T}(1{:}3,:)$ of the modified form of the 3 4-bar mechanisms with continuation

Furthermore, the diagonal coefficients of matrix $\mathbf{R}_1$ is displayed in Fig. 5.51.

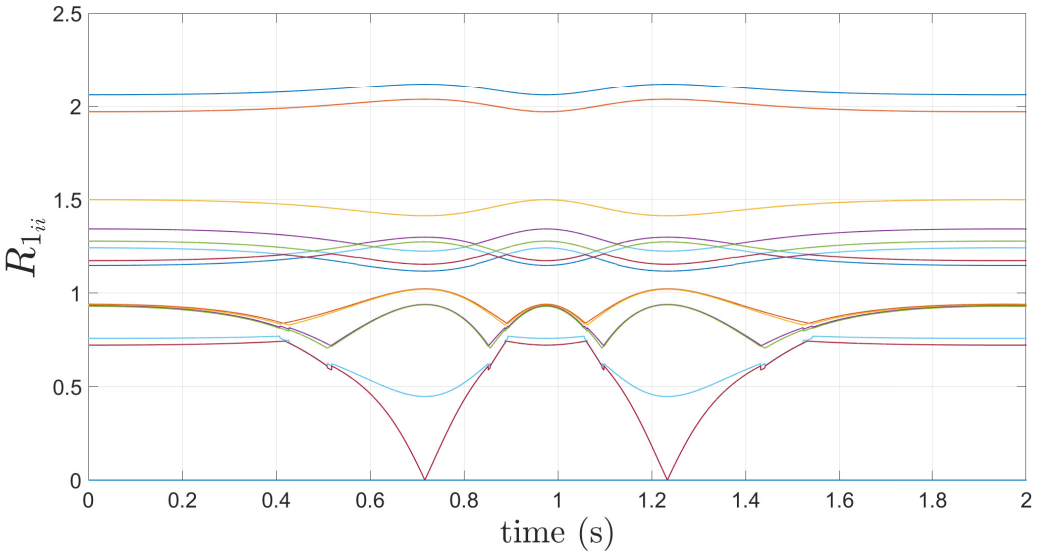

Figure 5.51: Time history of the diagonal values of matrix $\mathbf{R}_1$ of the modified form of the 3 4-bar mechanisms

The evaluation of matrix $\mathbf{T}$ when singularity occurred explains the possible motion of the system. Fig. 5.52 shows the values of $\mathbf{T}$ when singularity condition.

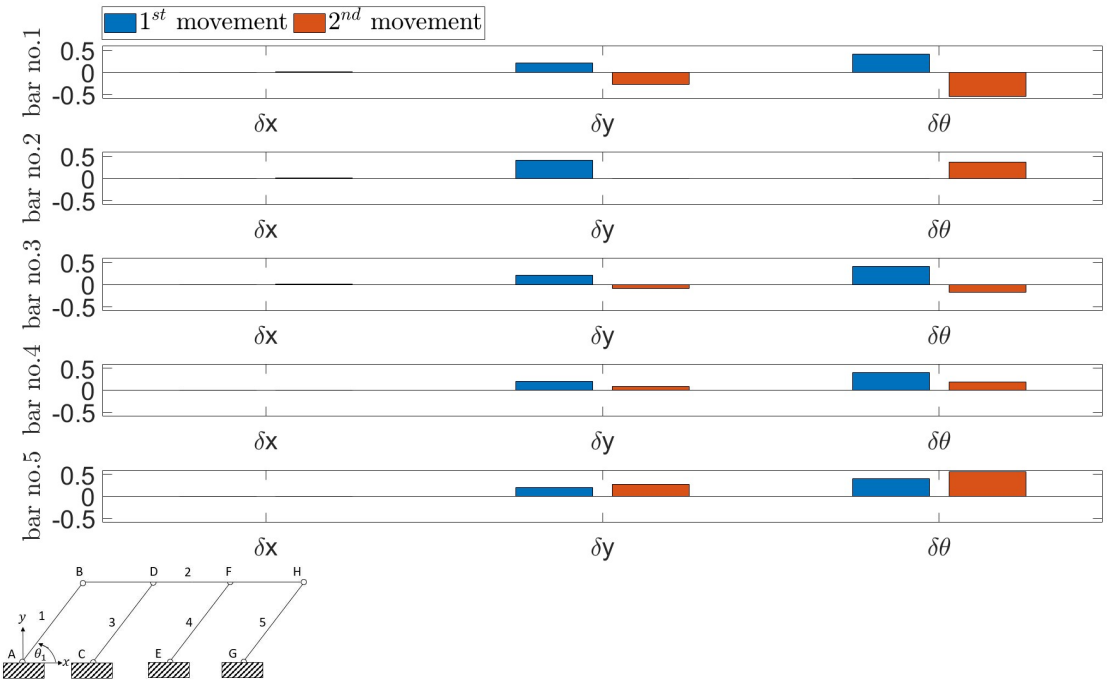

Figure 5.52: Possible movement of the modified form of the 3 4-bar mechanisms in the singularity condition

A more intuitive figure which shows the possible motion of all bars is displayed in Fig. 5.53.

(a) 1st movement

(b) 2nd movement

Figure 5.53: Possible movements of the modified form of the 3 4-bar mechanisms in the singularity condition

5.7. Modified Form of the 2×3 4-Bar Mechanisms

Modifying the 3 4-bar mechanisms by adding another 3 4-bar mechanisms with the same properties as the previous one. The system is given initial condition for θ_1 and θ_6 are equal with $\frac{\pi}{2}$. The initial angular velocities for bars number 2 and 7 is zero. The remaining bars have initial angular velocities of -1 rad/s.

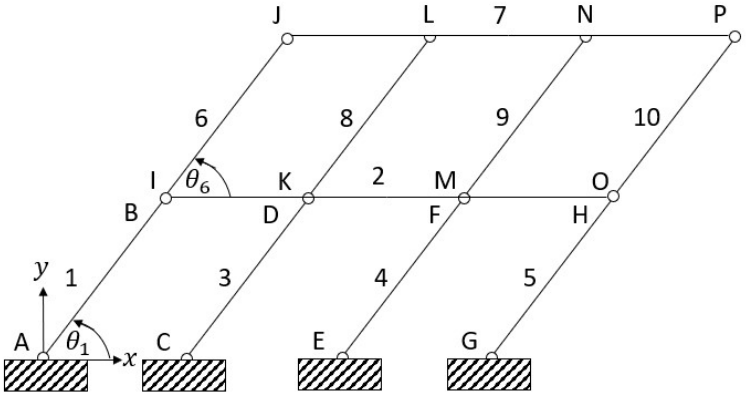

Figure 5.54: 2×3 4-bar mechanisms

The system is simulated for 2 seconds. The result for the position of bars number 1 and 6 is shown in Fig. 5.55.

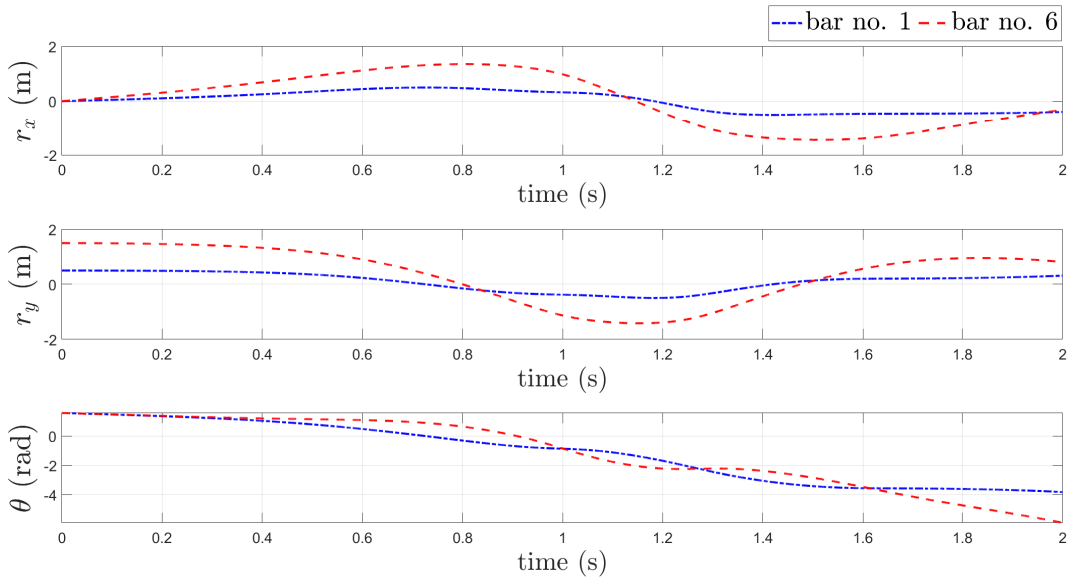

Figure 5.55: Time history of bars number 1 and 6 of the modified form of the 2×3 4-bar mechanisms

Furthermore, Fig. 5.56 shows the time history of the diagonal coefficients of matrix $\mathbf{R}_1$.

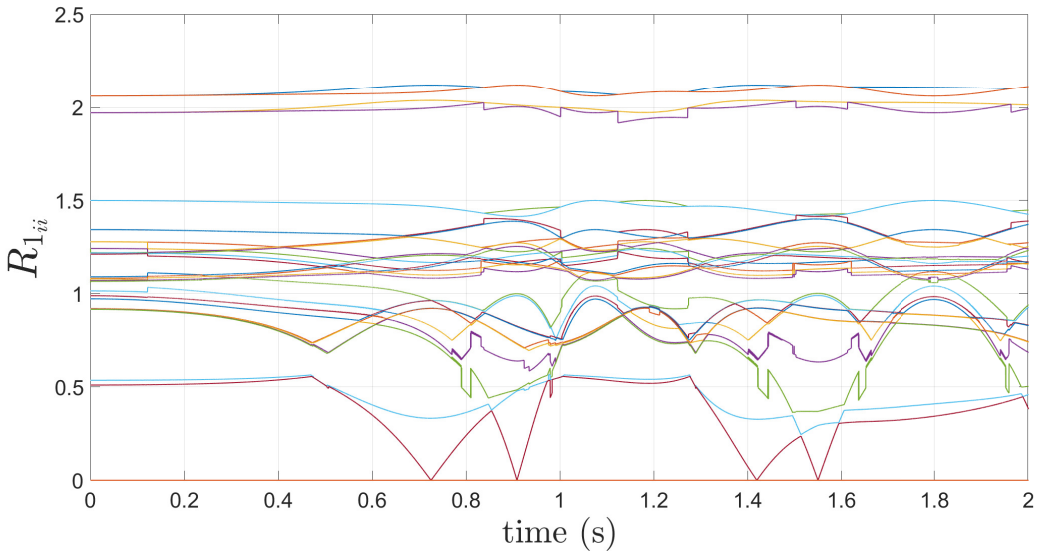

Figure 5.56: Time history of the diagonal values of matrix $\mathbf{R}_1$ of the modified form of the 2×3 4-bar mechanisms

It can be observed from Fig. 5.55 and Fig. 5.56 when singularity condition occurrs, a part of matrix $\mathbf{R}_1$ goes to zero. Between time 0.6 seconds and 1 second, the number of times matrix $\mathbf{R}_1$ goes to zeros is twice because the first part of the mechanism (bars number 1, 2, 3, 4, and 5) reached the horizontal positions at a different time from the second part

of the system (bars number 6, 7, 8, 9, and 10).

5.7.1. Continuation Algorithm for Modified Form of the 2×3 4-Bar Mechanisms

Applying the continuation algorithm to the 2×3 4-bar mechanisms results in the continuity of the generalized coordinates and projected generalized velocities. Fig. 5.57 shows the comparison of the generalized coordinates using traditional QR and continuation.

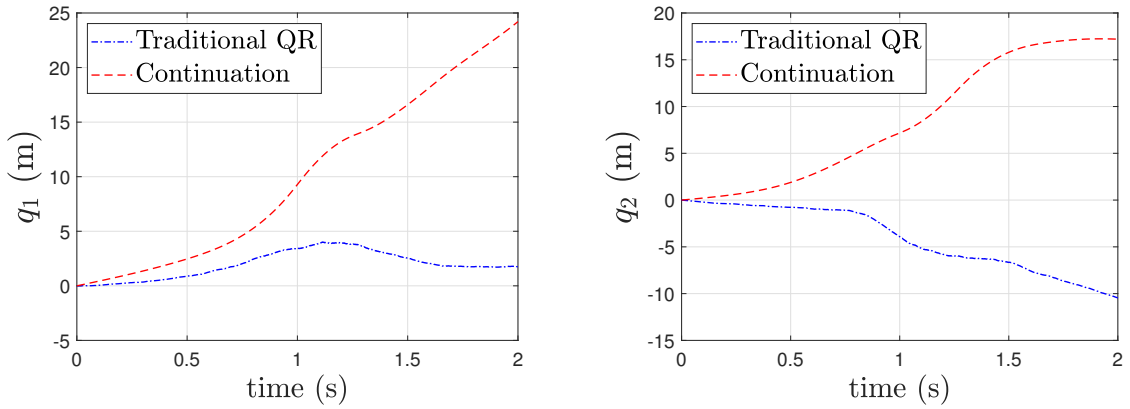

(a) Time history of q_1 (b) Time history of q_2

Figure 5.57: Time history of the generalized coordinates of the modified form of the 2×3 4-bar mechanisms

Furthermore, Fig. 5.58 shows the comparison of projected generalized velocities using traditional QR and continuation.

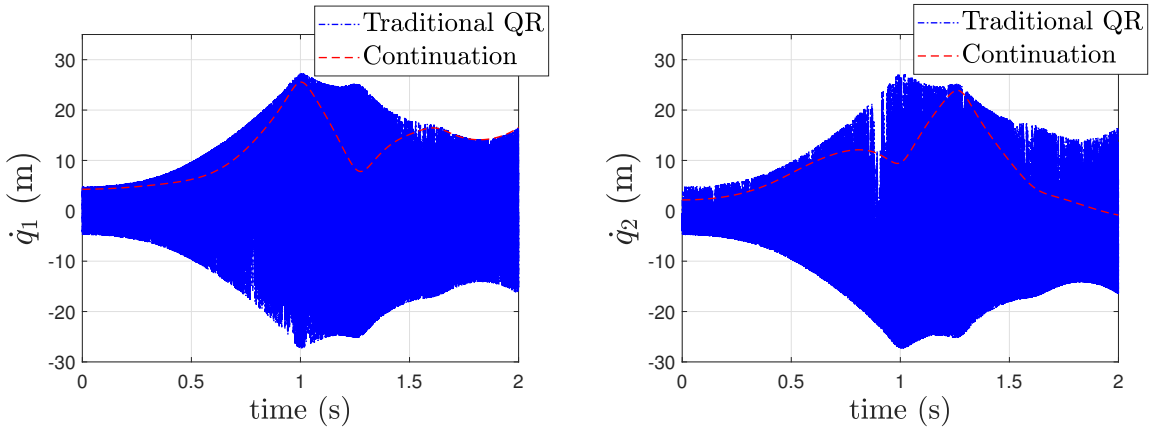

(a) Time history of $\dot{q}_1$ (b) Time history of $\dot{q}_2$

Figure 5.58: Time history of the projected velocities of the modified form of the 2×3 4-bar mechanisms

It can be observed from Fig. 5.57 and Fig. 5.58 that using the continuation, the values of the generalized coordinates and projected generalized velocities are continuous compared to using traditional QR.

6 | Conclusions

This thesis demonstrates the singularity detection and redundant constrained multibody system dynamics using the minimum coordinate set with the continuation algorithm. The computation is based on selecting an appropriate matrix. The matrix has to be tangent to constraint manifolds. This matrix is obtained from full QRP factorization of the constraint Jacobian matrix.

A singularity configuration occurs when the system experiences another possible motion regardless of its initial movement. Numerically, it can be seen by evaluating the coefficient of the diagonal matrix $\mathbf{R}_1$. When this condition occurs, some of the diagonal values of matrix $\mathbf{R}_1$ will go to zero, which leads to the rank deficiency of the constraint Jacobian matrix. This means that the matrix rank will decrease and result in the other possible motions of the system.

On the other hand, a system with a number of constraints greater or equal to the number of ordinary differential equations can perform a movement if the rank of matrix $\mathbf{A}$ is not-full, meaning some of the constraints are repeated. The number of admissible motions can be computed by subtracting the rank of matrix $\mathbf{A}$ from the smallest between the number of rows and columns.

Lastly, the continuation algorithm is used to create a regularity of the generalized coordinates. In other words, this method results in generalized coordinates which are continuous and differentiable, which is not the case for the traditional QR. On the contrary, it will not affect the physical coordinates, which means the results of the physical coordinates using the continuation are the same as traditional QR.

Several examples of mechanisms are presented. The first system consists of $m < n$ and a full-rank matrix A. The second system uses $m = n$ with redundant constraints. Lastly, a system with $m > n$ containing redundant constraints. The example of singularity is also presented in which the mechanism changes the motion by introducing a torque in the system.

Bibliography

[1] O. A. Bauchau and A. Laulusa. Review of contemporary approaches for constraint enforcement in multibody systems. *Journal of Computational and Nonlinear Dynamics*, 3(1), 2008.

[2] E. Bayo, J. G. de Jalón, and M. A. Serna. A modified lagrangian formulation for the dynamic analysis of constrained mechanical systems. *Applied Mechanics and Engineering*, 71:183–195, 1988.

[3] M. Borri, C. Bottasso, and P. Mantegazza. Equivalence of kane's and maggi's equations. *Meccanica*, 25:272–274, 1990.

[4] J. R. Dormand and P. J. Prince. A family of embedded runge-kutta formulae. *Journal of computational and applied mathematics*, 6(1):19–26, 1980.

[5] G. H. Golub and C. F. Van Loan. *Matrix computations*. JHU press, 2013.

[6] F. González, P. Masarati, J. Cuadrado, and M. A. Naya. Assessment of linearization approaches for multibody dynamics formulations. *Journal of Computational and Nonlinear Dynamics*, 12(4), 2017.

[7] E. J. Haug and J. Yen. Generalized coordinate partitioning methods for numerical integration of differential-algebraic equations of dynamics. In *Real-time integration methods for mechanical system simulation*, pages 97–114. Springer, 1991.

[8] Y. P. Hong and C.-T. Pan. Rank-revealing qr factorizations and the singular value decomposition. *Mathematics of Computation*, 58(197):213–232, 1992.

[9] T. R. Kane and C. Wang. On the derivation of equations of motion. *Journal of the Society for Industrial and Applied Mathematics*, 13(2):487–492, 1965.

[10] A. Laulusa and O. A. Bauchau. Review of classical approaches for constraint enforcement in multibody systems. *Journal of computational and nonlinear dynamics*, 3(1), 2008.

[11] G. A. Maggi. *Principii della teoria matematica del movimento dei corpi: corso di meccanica razionale*. Ulrico Hoepli, 1896.

[12] G. A. Maggi. *Principii di stereodinamica: corso sulla formazione, l'interpretazione e l'integrazione delle equazioni del movimento dei solidi*. U. Hoepli, 1903.

[13] N. K. Mani, E. J. Haug, and K. E. Atkinson. Application of Singular Value Decomposition for Analysis of Mechanical System Dynamics. *Journal of Mechanisms, Transmissions, and Automation in Design*, 107(1):82–87, 03 1985. ISSN 0738-0666. doi: 10.1115/1.3258699.

[14] L. Mariti, N. P. Belfiore, E. Pennestrì, and P. P. Valentini. Comparison of solution strategies for multibody dynamics equations. *International Journal for Numerical Methods in Engineering*, 88(7):637–656, 2011.

[15] P. Masarati. Adding kinematic constraints to purely differential dynamics. *Computational Mechanics*, 47:187–203, 2011.

[16] P. Masarati, M. J. U. Quro, and A. Zanoni. Projection continuation for minimal coordinate set formulation and singularity detection of redundantly constrained system dynamics. In *Multibody System Dynamics*. Springer, 2023. submitted.

[17] H. Munthe-Kaas. High order runge-kutta methods on manifolds. *Applied Numerical Mathematics*, 29(1):115–127, 1999.

[18] E. C. Steeves and W. Walton Jr. A new matrix theorem and its application for establishing independent coordinates for complex dynamical systems with constraints. Technical report, TR R-326, NASA, 1969.

[19] C. F. Van Loan. Generalizing the singular value decomposition. *SIAM Journal on numerical Analysis*, 13(1):76–83, 1976.

[20] R. A. Wehage and E. J. Haug. Generalized Coordinate Partitioning for Dimension Reduction in Analysis of Constrained Dynamic Systems. *Journal of Mechanical Design*, 104(1):247–255, 01 1982. ISSN 0161-8458. doi: 10.1115/1.3256318.

[21] H. Zhang, R. Zhang, and P. Masarati. Improved second-order unconditionally stable schemes of linear multi-step and equivalent single-step integration methods. *Computational Mechanics*, 67:289–313, 2021.

[22] H. Zhang, R. Zhang, A. Zanoni, and P. Masarati. Performance of implicit a-stable time integration methods for multibody system dynamics. *Multibody System Dynamics*, 54(3):263–301, 2022.

[23] P. Zhou, A. Zanoni, and P. Masarati. A projection continuation approach for minimal coordinate set constrained dynamics. *Multibody System Dynamics*, pages 1–21, 2023.

A | Reorthogonalization After Continuation

For convenience, the reorthogonalization will be explained for the specific cases, namely $m < n$ and $d > 0$. Even so, this method can still be used for other problems, such as systems with $m > n$ and $d > 0$ or systems with no redundant constraints.

Considering $\tilde{\mathbf{T}}$ is the suitable subspace matrix obtained from the continuation and $\hat{\mathbf{T}}$ is the suitable subspace matrix from QR factorization. As mentioned before, the two matrices may differ due to the accumulation of numerical errors during the integration, including the correction of physical coordinates to bring them back onto the constraint manifold. Matrix $\mathbf{T}$ after orthogonalized must consist of

1. a recombination of matrix $\hat{\mathbf{T}}$,
2. as close as possible to $\tilde{\mathbf{T}}$

To do that, some processes must be followed.

The first requirement could be done by multiplication with matrix $\mathbf{P}$

$$\mathbf{T} = \hat{\mathbf{T}}\mathbf{P} \tag{A.1}$$

Matrix $\mathbf{P} \in \mathbb{R}^{(n-m+d)\times(n-m+d)}$ is orthonormal matrix, i.e. subjected to the constraint

$$\mathbf{P}\mathbf{P}^T = \mathbf{I} \tag{A.2}$$

such that

$$\mathbf{T}^T\mathbf{T} = \mathbf{P}^T\hat{\mathbf{T}}^T\hat{\mathbf{T}}\mathbf{P} = \mathbf{P}^T\mathbf{P} = \mathbf{I} \tag{A.3}$$

The second requirement is met by determining matrix $\mathbf{P}$ subjected to the condition,

$$\min_{\mathbf{P}} \|\tilde{\mathbf{T}}^T \mathbf{T} - \mathbf{I}\| \tag{A.4}$$

where $\|.\|$ indicates a suitable matrix norm that will be defined later.

Consider matrix $\mathbf{E}$ as,

$$\mathbf{E} = \tilde{\mathbf{T}}^T \mathbf{T} - \mathbf{I} = \mathbf{CP} - \mathbf{I} \tag{A.5}$$

such that,

$$\mathbf{C} = \tilde{\mathbf{T}}^T \hat{\mathbf{T}} \tag{A.6}$$

That problem in Eq. (A.4) can be remodeled as a minimization of the cost function J that is defined as a square of Frobenius norm of matrix $\mathbf{E}$ with respect to matrix $\mathbf{P}$, subjected to the constraint of Eq. (A.2). It can be done by transforming the constraint minimization into an unconstrained one with the addition of the constraint equation to the cost function using the Lagrange multipliers, $\mathbf{\Lambda} \in \mathbb{R}^{(n-m+d)\times(n-m+d)}$.

$$J = \mathrm{tr}((\mathbf{CP} - \mathbf{I})(\mathbf{CP} - \mathbf{I})^T) + \mathrm{tr}\left((\mathbf{PP}^T - \mathbf{I})\mathbf{\Lambda}\right) \tag{A.7}$$

The stationary condition can be evaluated by taking the partial derivative of cost function J related to the minimization variables equal to zero. Setting the partial derivative of J concerning $\mathbf{\Lambda}$ equal to $\mathbf{0}$ yields the constraint equation, Eq. (A.2). On the other hand, setting the partial derivative of J regarding $\mathbf{P}$ equal to $\mathbf{0}$ yields the equations as follows

$$\frac{\partial J}{\partial \mathbf{P}} = 2\mathbf{C}^T(\mathbf{CP} - \mathbf{I}) + 2\mathbf{\Lambda P} = \mathbf{0} \tag{A.8}$$

such that,

$$\mathbf{P}^{-1} = \mathbf{C}^{-T}(\mathbf{C}^T\mathbf{C} + \mathbf{\Lambda}) = \mathbf{P}^T \tag{A.9}$$

Substituting Eq. (A.9) equation to Eq. (A.2) yields

$$\mathbf{\Lambda} + \mathbf{\Lambda}^T + \mathbf{\Lambda}^T\mathbf{C}^{-1}\mathbf{C}^{-T}\mathbf{\Lambda} + \mathbf{C}^T\mathbf{C} - \mathbf{I} = \mathbf{0} \tag{A.10}$$

Eq. (A.10) is acquainted as a continuation algebraic Riccati in $\mathbf{\Lambda}$. Solving that equation yields $\mathbf{\Lambda}$ and substituting $\mathbf{\Lambda}$ in Eq. (A.9) to get

$$\mathbf{P} = (\mathbf{C}^T\mathbf{C} + \mathbf{\Lambda})\mathbf{C}^{-1} \tag{A.11}$$

Thus, the suitable matrix $\mathbf{T}$ after reorthogonalization can be obtained from the Eq. (A.1).

Alternatively, based on the polar decomposition theorem, matrix $\mathbf{C}^T$ can be decomposed into the product of the orthonormal matrix $\mathbf{U} \in \mathbb{R}^{(n-m+d)\times(n-m+d)}$ and the symmetric matrix, positive (semi)definite, $\mathbf{D} \in \mathbb{R}^{(n-m+d)\times(n-m+d)}$, i.e.

$$\mathbf{C}\mathbf{C}^T = \mathbf{D}^T\mathbf{U}^T\mathbf{U}\mathbf{D} = \mathbf{D}^T\mathbf{D} \overset{sym.}{=} \mathbf{D}^2 \tag{A.12}$$

So, it can be rewritten as

$$\mathbf{D} = (\mathbf{C}\mathbf{C}^T)^{\frac{1}{2}} \tag{A.13}$$

where operation $(.)^{\frac{1}{2}}$ shows a square root operation of matrix and thus

$$\mathbf{U} = \mathbf{C}^T\mathbf{D}^{-1} \tag{A.14}$$

Matrix U corresponds to the optimal matrix of Eq. (A.11).

The proof is done by showing that the value of the cost function J will be minimal when $\mathbf{P} \equiv \mathbf{U}$. Assume that $\mathbf{P}$ comes from matrix $\mathbf{U}$ multiplied by any orthogonal matrix.

$$\mathbf{P} = \mathbf{U}\mathbf{W} \tag{A.15}$$

where $\mathbf{W} \in \mathbb{R}^{(n-m+d)\times(n-m+d)}$ is an arbritary orthogonal matrix, so that $\mathbf{W}^T\mathbf{W} \equiv \mathbf{I}$. Therefore, matrix $\mathbf{P}$ will satisfy the constraint in Eq.(A.2). Thus, requirement number 1 is guaranteed.

Substituting Eq. (A.15) to cost function J, Eq. (A.7). Thus,

$$J_{\mathbf{W}} = \mathrm{tr}(\mathbf{D}^2 - \mathbf{D}\mathbf{W} - \mathbf{W}^T\mathbf{D} + \mathbf{I}) \tag{A.16}$$

Exploiting the fact that $\mathrm{tr}(\mathbf{M}^T) = \mathrm{tr}(\mathbf{M})$,

$$J_{\mathbf{W}} = \mathrm{tr}(\mathbf{D}^2 - 2\mathbf{D}\mathbf{W} + \mathbf{I}) \tag{A.17}$$

The variation of cost function J is formulated as

$$\begin{aligned} J_{\mathbf{W}} - J_{\mathbf{W}\equiv\mathbf{I}} &= \mathrm{tr}(\mathbf{D}^2 - 2\mathbf{D}\mathbf{W} + \mathbf{I}) - \mathrm{tr}(\mathbf{D}^2 - 2\mathbf{D} + \mathbf{I}) \\ &= 2\mathrm{tr}(\mathbf{D}(\mathbf{I} - \mathbf{W})) \end{aligned} \tag{A.18}$$

Without losing generality, the easiest possible perturbation matrix for $\mathbf{W}$ is one consisting of the 2D rotational equivalents of the first two directions in the coordinate space, i.e.

$$\mathbf{W} = \begin{bmatrix} \cos\theta & -\sin\theta & 0 & \dots & 0 \\ \sin\theta & \cos\theta & 0 & \dots & 0 \\ 0 & 0 & 1 & \dots & 0 \\ \vdots & \vdots & \vdots & \ddots & \vdots \\ 0 & 0 & 0 & \dots & 0 \end{bmatrix} \tag{A.19}$$

Thus, matrix $\mathbf{D}\mathbf{W}$ can be write as follows

$$\mathbf{D}\mathbf{W} = \begin{bmatrix} D_{11}\cos\theta + D_{12}\sin\theta & & & \dots & (\text{irrelevant}) \\ & -D_{12}\sin\theta + D_{22}\cos\theta & & \dots & \\ & & D_{33} & \dots & \\ \vdots & \vdots & \vdots & \ddots & \vdots \\ (\text{irrelevant}) & & & \dots & D_{(n-m+d)(n-m+d)} \end{bmatrix} \tag{A.20}$$

taking advantage of the symmetry matrix $\mathbf{D}$, its trace is

$$\begin{aligned} \mathbf{D}\mathbf{W} &= D_{11}\cos\theta + D_{12}\sin\theta - D_{12}\sin\theta + D_{22}\cos\theta + \sum_{i=3}^{n-m+d} D_{ii} \\ &= (D_{11} + D_{22})\cos\theta + \sum_{i=3}^{n-m+d} D_{ii} \end{aligned} \tag{A.21}$$

Which is smaller than or at most equal to the trace $\mathbf{D}$ alone, because $\cos\theta \leq 0 \, \forall\theta$, yielding

$$J_{\mathbf{W}} - J_{\mathbf{W}\equiv\mathbf{I}} = 2\mathrm{tr}(\mathbf{D}(\mathbf{I} - \mathbf{W})) = 2(D_{11} + D_{22})(1 - \cos\theta) \leq 0 \tag{A.22}$$

This is a second-order variation with respect to the perturbation: for $|\theta| \ll 1$, $\cos\theta \approx 1 - \theta^2/2$, thus

$$J_{\mathbf{W}} - J_{\mathbf{W}\equiv\mathbf{I}} \approx (D_{11} + D_{22})\theta^2 \tag{A.23}$$

i.e. $\theta \equiv 0$ represents a minimum.

Since an arbitrary perturbation can be transformed into an alternative formulation via a suitable coordinate transformation, this proves the optimality of that proposed approach. Also, since the same cost function of the original case was used, this proves their equality.

List of Figures

List of Tables

Acknowledgements

First and foremost, I would like to express my heartfelt thanks to my advisor, Professor Pierangelo Masarati, who provided a chance to work together and helped me finish my thesis. Under his supervision, I received unwavering support and encouragement that allowed me to focus on my research and academic success. His guidance and advice were invaluable to completing this work and shaping my academic and professional growth.

Furthermore, I extend my sincerest gratitude to my parents and teacher in Indonesia for providing support and motivation throughout my years of study. Their unconditional love was crucial in allowing me to overcome challenges or doubts during my work.

I would also like to thank my friends and companions, Dimas, Irfan, Soufiane, and Zakaria, who encouraged me throughout my journey. Their understanding and assistance were a positive source of inspiration for me, and I will forever cherish their friendship.

Lastly, my heartfelt thanks go to Politecnico di Milano for awarding me with a scholarship for my master's study. Their financial support enabled me to focus on my creative facet and scholastic career. This journey was like a rollercoaster for me, physically and emotionally. I am very grateful for meeting people from all over the world and experiencing new cultures.